HHS Public Access

Author manuscript

Cell. Author manuscript; available in PMC 2018 November 02.

Published in final edited form as:

Cell. 2017 November 02; 171(4): 771–782.e11. doi:10.1016/j.cell.2017.09.051.

The human knockout gene CLYBL connects itaconate to vitamin B12

Hongying Shen[1,2,3], **Gregory Campanello**[4], **Daniel Flicker**[1,2,3], **Zenon Grabarek**[1,2,3], **Junchi Hu**[5], **Cheng Luo**[5], **Ruma Banerjee**[4], and **Vamsi K. Mootha**[1,2,3,6,*]

[1]Howard Hughes Medical Institute and Department of Molecular Biology, Massachusetts General Hospital, Boston, MA 02114, USA

[2]Department of Systems Biology, Harvard Medical School, Boston, MA 02115, USA

[3]Broad Institute, Cambridge, MA 02141, USA

[4]Department of Biological Chemistry, University of Michigan Medical School, Ann Arbor, MI 48109, USA

[5]Drug Discovery and Design Center, State Key Laboratory of Drug Research, Shanghai Institute of Materia Medica, Chinese Academy of Sciences, Shanghai 200031, China

Summary

CLYBL encodes a ubiquitously expressed mitochondrial enzyme, conserved across all vertebrates, whose cellular activity and pathway assignment are unknown. Its homozygous loss is tolerated in seemingly healthy individuals, with reduced circulating B_{12} levels being the only and consistent phenotype reported to date. Here, by combining enzymology, structural biology and activity-based metabolomics we report that CLYBL operates as a citramalyl-CoA lyase in mammalian cells. Cells lacking CLYBL accumulate citramalyl-CoA, an intermediate in the C5-dicarboxylate metabolic pathway that includes itaconate, a recently identified human antimicrobial metabolite and immunomodulator. We report that CLYBL loss leads to a cell autonomous defect in the mitochondrial B_{12} metabolism and that itaconyl-CoA is a cofactor-inactivating, substrate-analogue inhibitor of the mitochondrial B_{12}-dependent methylmalonyl-CoA mutase (MUT). Our work de-orphans the function of human CLYBL and reveals that a consequence of exposure to the immunomodulatory metabolite itaconate is B_{12} inactivation.

eTOC

*Correspondence: vamsi@hms.harvard.edu.
6Lead Contact

Author contributions

H.S. and V.K.M. initiated the project and interpreted the data. H.S. and D.F. performed the cell-based studies. H.S. and G.C. performed the biochemical experiments. H.S. and Z.G. performed the structural analysis. J.H. and L.C. performed the structural docking. H.S. and V.K.M. wrote the manuscript. G.C., Z.G., and R.B. edited the manuscript.

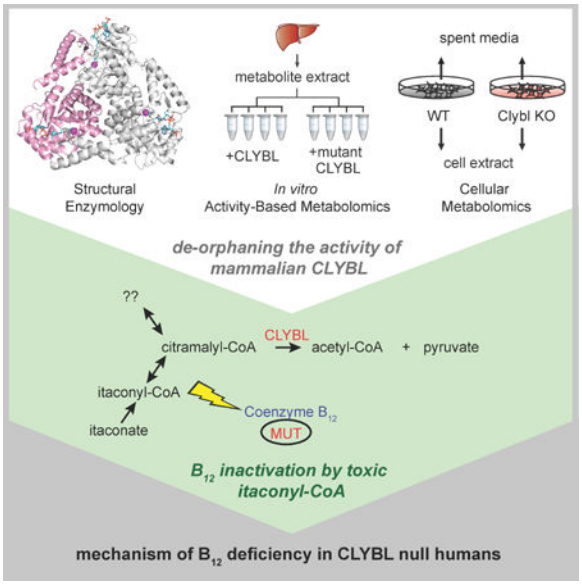

A human missing gene sheds light into how production of itaconate, an immunometabolite, may contribute to vitamin B12 deficiency

Introduction

CLYBL is one of a small but growing class of polymorphic human genes that harbors bi-allelic, loss of function (LoF) variants in seemingly healthy individuals. This collection of genes includes *ALDH2* (whose LoF confers flushing in response to alcohol), *PCSK9* (whose LoF protects against cardiovascular disease), and *CCR5* (an HIV co-receptor whose mutation confers resistance to AIDS). Such genes are of outstanding clinical relevance and have historically provided valuable insights into human evolution and physiology with implications for therapeutics development (Harper et al., 2015).

In the case of CLYBL, its loss is found in 2.7 % of all human chromosomes due to a single nucleotide polymorphism (SNP rs41281112) that changes Arg259 to a stop codon and leads to loss of the protein. While this LoF SNP is found in East Asian, Europeans, Latinos and South Asians, it is rare (0.57 %) in Africans (Lek et al., 2016). Recently, three independent GWAS studies found that homozygosity of this mutation is associated with a strong reduction of circulating B_{12} in otherwise seemingly healthy people (Grarup et al., 2013; Lim et al., 2014; Lin et al., 2012). Previous computational analysis performed in our laboratory found that CLYBL is co-evolved and co-expressed with genes involved in mitochondrial B_{12} processing (MMAB and MMAA) and B_{12} -dependent activity (MUT) (Strittmatter et al., 2014).

CLYBL is a ubiquitously expressed mitochondrial matrix soluble enzyme of unknown function (Calvo et al., 2016). It is annotated as “Citrate lyase subunit beta-like protein,” due to its homology to bacterial *cit*E, β-subunit of bacterial citrate lyase that cleaves citrate to oxaloacetate and acetyl-CoA (Dimroth and Eggerer, 1975). However, mammals lack other essential subunits of the citrate lyase enzyme complex suggesting an alternative enzymatic

activity for CLYBL. Previously, our laboratory was the first to report *in vitro* enzymatic activity of human CLYBL and demonstrated a modest but specific malate/methylmalate synthase activity, as well as a much weaker citramalate synthase activity (Strittmatter et al., 2014). A partial reverse *in vitro* activity of CLYBL to cleave citramalyl-CoA (CoA ester of citramalate) into pyruvate and acetyl-CoA has been reported in a study that focused on the bacterial ortholog of CLYBL (Sasikaran et al., 2014). The *in vivo* enzymatic activity, the physiological role of the activities, if any, and the connection to B_{12} have remained unexplored.

Vitamin B_{12}, also known as cobalamin (Cbl), is an essential cofactor in humans that we obtain from our diet (Banerjee et al., 2009; Gherasim et al., 2013). Severe B_{12} deficiency is associated with anemia and neurological impairments, while mild B_{12} deficiency is very common. Only two human enzymes use B_{12} as a cofactor: methionine synthase (MTR) and methylmalonyl-CoA mutase (MUT). The cytosolic enzyme MTR utilizes the methyl group of methylcobalamin (MeCbl) to synthesize methionine from homocysteine. MUT is a mitochondrial matrix enzyme that uses coenzyme B_{12} or 5´-adenosylcobalamin (AdoCbl) as the cofactor. It catalyzes the conversion of methylmalonyl-CoA into succinyl-CoA, which allows recycling of branched carbon chains from amino acids and lipids into the tricarboxylic acid cycle (TCA cycle). AdoCbl is synthesized by a known matrix cobalamin adenosyltransferase MMAB; and another matrix GTPase MMAA is required for cofactor loading into the MUT enzyme.

Much of what we know about cellular B_{12} function has come from investigating patients with impaired B_{12} metabolism. To date, mutations in genes for 10 cellular complementation groups based on patient-derived fibroblasts have been identified, thereby providing insight into the intracellular trafficking and biochemistry of B_{12} (Watkins and Rosenblatt, 2011, 2016). A recent GWAS studies for low circulating B_{12} levels in human have revealed its association with 11 loci (Grarup et al., 2013). The function of nearly all of the loci-harboring genes and their relationship to B_{12} are known, with *CLYBL* being a notable exception.

Here, by combining genome editing, structural biology, activity-based metabolite profiling and detailed enzymology, we have determined the *in vivo* enzymatic activity of mammalian CLYBL, and identified its role in C5 dicarboxylate catabolism. Our study reveals a novel mechanism by which itaconyl-CoA, an intermediate in itaconate catabolism, directly inhibits B_{12} -dependent MUT enzyme by inactivating the coenzyme B_{12} cofactor. Our work defines the function of the missing human gene CLYBL, and also explains how its loss leads to low B_{12} levels in humans via a novel mechanism of B_{12} toxicity. An implication of our study is that, during immune activation, itaconate produced at a high concentration by macrophages might cause a B_{12} deficiency, pointing to an unexpected link between immunity and vitamin B_{12}.

Results

Assaying the forward and reverse activities of CLYBL

Previous studies from our laboratory have reported a forward activity for CLYBL *in vitro* to synthesize malate, methylmalate and citramalate (Strittmatter et al., 2014), while a partial

reverse citramalyl-CoA lyase activity has also been reported (Sasikaran et al., 2014). To our knowledge, these forward and reverse activities have not been jointly tested to enable a head to head comparison. Here, we used HPLC-UV detection method for CoA esters to directly compare the forward and the reverse enzymatic activity for the recombinant human CLYBL enzyme. Using this method, we directly examined all putative reactions shown in Figure 1A and found that CLYBL has a very high and specific citramalyl-CoA lyase activity. The K_M value for citramalyl-CoA is comparable to the K_M values for acetyl-CoA or propionyl-CoA, the substrates in the forward reaction, probably because substrate binding is primarily driven by the electrostatic interactions between the protein and the CoA moiety. The specificity constant (k_{cat}/K_M) for the citramalyl-CoA lyase activity is >1000 fold higher than the forward malate/methylmalate/citramalate synthase activity (Figure 1B). We also found that CLYBL has a thioesterase activity and hydrolyzes malyl-CoA to malate and free CoASH, but we did not quantify this activity in detail. We failed to detect dimethylmalate/dimethylmalyl-CoA synthase, malyl-CoA lyase and methylmalyl-CoA lyase activities.

Structural analysis of CLYBL

We solved the crystal structure of the full length human CLYBL protein lacking the predicted mitochondrial targeting sequence (aa 23 – 340), both in *apo* form (at 3.0 Å resolution) and in complex with either CoASH (at 1.9 Å resolution, formate-form) or with propionyl-CoA (Pro-CoA) (at 2.3 Å resolution, PEG-form) (Figure 1C and Table S1). Pro-CoA is the substrate for the forward reaction to generate methylmalate, so it was used in the crystallization condition to produce substrate-bound structure, as citramalyl-CoA cannot be produced in high yields using our enzymatic synthesis method.

Our crystal structures provide important information regarding the potential enzymatic mechanism of CLYBL. CLYBL is a homotrimer in the presence or absence of substrate analogs (Figure S1A). The CLYBL structures in the two substrate-analog-bound forms (complex-formate with CoASH and complex-PEG with Pro-CoA) are almost identical, and the only difference is the lack of Mg^{2+} in the active site, that most likely was extracted by the high concentration of citrate in the crystallization condition for the PEG form. Substrate mimics, Pro-CoA or free CoASH, are bound in a cavity at the interface between the N terminal domain of one subunit and the C terminal region of the next subunit of the homotrimer, which defines the catalytic site (Figure 1C and Figure S1B and C). While the N terminal domain of CLYBL shows high sequence similarity with the bacterial citrate lyase β subunit orthologs for which crystal structures are available, the C terminal segment of CLYBL lacks sequence similarity with homologous proteins with known structures. The N-terminal domain forms a characteristic $\beta_8\alpha_8$-TIM barrel fold. The C-terminal 50 residues form a lid domain consisting of two helices connected by a β-hairpin loop. It is connected to the TIM barrel via a short flexible linker. The C terminal lid domain is of particular interest. By comparing the apo- and substrate-bound forms of CLYBL, we observed that the lid domain swivels in and out of the active site, moving in to cover the substrate via interactions with the CoA moiety (Figure S1A).

Based on the crystal structures, we designed a catalytic mutant of CLYBL for functional studies. Previously, we had predicted that a highly conserved Asp320 residue located in the

C-terminal lid domain might be critical for CLYBL's activity (Strittmatter et al., 2014), because a remote bacterial ortholog of CLYBL, malate synthase, also contains a structurally equivalent aspartate residue that is critical for abstracting a proton from the substrate and stabilizing the enol intermediate during the catalytic cycle (Bracken et al., 2011; Zarzycki and Kerfeld, 2013). Asp320 is located at the base of the β-hairpin in the C-terminal lid domain. Mutating this aspartate residue to asparagine or alanine abolishes the malate synthase activity (Zarzycki and Kerfeld, 2013). In the case of CLYBL, a similar enol structure is the necessary intermediate for both the forward and the partial reverse citramalyl-CoA lyase reaction. Our CLYBL structure confirmed that the Asp320 residue on the C terminal domain in one subunit is indeed very close to the CoA bound at the subunit interface (Figure 1C). Consistently, we did not detect any citramalyl-CoA lyase activity with the CLYBL^{D320N} and CLYBL^{D320A} mutants (Figure S1G).

We used two additional strategies – one *in silico*, one *in vitro*-to determine if CLYBL might support additional enzymatic activities. First, we docked the substrate (*S*)-citramalyl-CoA into the Pro-CoA-bound crystal structure of CLYBL (Figure 1D). The methyl group on the citramalyl-CoA is in close proximity to the side chains of several amino acids from CLYBL, preventing accommodation of additional carbon atoms in analogues larger than citramalyl-CoA (Figure 1E). Second, we adopted an *in vitro* activity-based metabolite profiling method (de Carvalho et al., 2010), and systematically probed the substrates/products that wild-type and mutant CLYBLs could act on. We purified recombinant human CLYBL and the catalytically inactive CLYBL^{D320N} mutant, incubated the enzymes in a rich metabolite extract from mouse livers for four time points, and then performed untargeted metabolic profiling for polar metabolites (Figure S1D and Table S2). When we compared CLYBL^{WT} and CLYBL^{D320N} sample at 60 min, two metabolites showed significant differences: acetyl-CoA and citramalate/methylmalate (indistinguishable isomers) (Figure S1E). Both peaks showed consistent changes with time (Figure S1F). The decrease in acetyl-CoA level and the increase in citramalate/methylmalate level suggests that CLYBL has citramalate synthase activity under these *in vitro* conditions, consistent with previous *in vitro* enzymatic studies (Strittmatter et al., 2014).

CLYBL functions as a citramalyl-CoA lyase in living cells

The *in vitro* enzymatic activity and structural considerations suggest that citramalate synthase and citramalyl-CoA lyase activities are likely the most relevant forward and reverse activities of the enzyme, with the directionality most likely being in the lyase direction but dependent on prevailing intracellular metabolite concentrations. If this hypothesis is true, then knocking out CLYBL should lead to accumulation of citramalyl-CoA in living cells.

We sought to identify a cellular model in which to investigate loss-of-function of CLYBL. When analyzing murine tissue expression profile (BioGPS) (Wu et al., 2016; Wu et al., 2013), we found that mouse *Clybl* is ubiquitously expressed, with the highest expression in the brown adipose. Protein products of mouse *Clybl* and human *CLYBL* share high sequence similarity (86 % identity). We utilized a previously reported immortalized murine brown adipocyte cell line (Pan et al., 2009) and confirmed that Clybl expression is highly induced after differentiation in culture (Figure S2A). We then generated Clybl CRISPR

knockout brown preadipocytes using pooled lentivirus carrying two sgRNA guides targeting the coding regions in exon 1 and exon 2 (Figure 3A). Clybl CRISPR knockout (KO) preadipocytes grow normally. The differentiated Clybl KO brown adipocytes express high levels of *Ucp1*, *Ppargc1a* and *Uqcrc1*, genes known to be highly expressed in brown adipocytes (Figure S2B), and form clusters of small lipid droplets that are indistinguishable from those in WT cells (Figure S2C). KO cells also show normal mitochondrial bioenergetics, including normal baseline and maximum (uncoupled) oxygen consumption rates (Figure S2D–F). Hence, loss of Clybl appears to be tolerated in this cell line, perhaps not surprising since humans can tolerate homozygous loss of CLYBL.

To directly assay the concentration of citramalyl-CoA in cultured cells, we developed a high-resolution LC-MS method for detecting CoA esters including citramalyl-CoA. While citramalyl-CoA is not detected in a highly concentrated wild-type cellular metabolite extract, it is accumulated in such extracts from Clybl KO brown adipocytes (Figure 2A). It is worth noting that as citramalyl-CoA is of very low abundance, we had to concentrate the cellular extract samples 100-fold, in comparison to the polar metabolite extractions that we normally performed for our typical metabolite profiling experiments. Accumulation of citramalyl-CoA in the Clybl KO cells helps to establish the directionality of the CLYBL reaction and supports the conclusion that CLYBL functions as a citramalyl-CoA lyase in living cells.

CLYBL operates in C5 dicarboxylate metabolism

We next sought to identify the metabolic pathway within which CLYBL might be operating. Citramalyl-CoA is an obscure metabolite within the context of mammalian metabolism. Studies in the 1960's reported that mouse liver extracts can metabolize five carbon (C5) dicarboxylates (including methylsuccinate, itaconate and mesaconate) in a three-step pathway, in which the last step is catalyzed by citramalyl-CoA lyase, an enzyme whose activity was detected but whose identity was unknown (Adler et al., 1957; Wang et al., 1961). More recent studies have shown that activated macrophages can generate itaconate, an anti-microbial metabolite, in millimolar concentrations (Jha et al., 2015; Michelucci et al., 2013; Strelko et al., 2011). In principle itaconate can be converted to itaconyl-CoA and citramalyl-CoA via the previously reported reversible hydration reaction catalyzed by methylglutaconyl-CoA hydratase (AUH) (Wang et al., 1961). Recently, a similar pathway has been indicated as mechanism utilized by some pathogens, such as *Yersinia pestis* and *Pseudomonas aeruginosa*, for survival in macrophages (Sasikaran et al., 2014). Together, these observations led us to speculate that CLYBL might be operating in the C5-dicarboxylate metabolic pathway (Figure 2C).

We sought to test if the CLYBL substrate citramalyl-CoA could be derived from itaconate. First, we observed a dramatic increase in citramalyl-CoA levels in wild-type brown fat cells exposed to 2 mM itaconate (Figure 2B). Second, when the culture medium was supplemented with 1 mM uniformly labeled itaconate-$^{13}C_5$ (Figure 2D and 2E), the citramalyl-CoA detected in cellular extracts was predominantly labeled as the M+5 species (Figure 2F), consistent with its production from itaconate (Figure 2C). Our experiment demonstrates that, in brown adipocytes, the catabolic pathway from itaconate to citramalyl-

CoA is indeed active. This experiment does not however, rule out the possibility of additional sources of citramalyl-CoA, for instance methylsuccinate and mesaconate.

Clybl loss leads to a cell-autonomous defect in mitochondrial B_{12} metabolism

Loss of CLYBL in humans leads to reduced circulating levels of B_{12}, but a key question is whether this is a cell autonomous effect, since many genes associated with reduced B_{12} levels are related to B_{12} absorption from the gut and its transport in circulation.

To identify metabolic changes in the Clybl KO brown fat cells, we performed untargeted LC-MS based metabolic profiling experiments to analyze polar metabolites in the 3 day spent media and cellular extract (Figure 3B). Full scan metabolic analysis of KO and WT cells revealed that several ions with mass-to-charge ratio (m/z) corresponding to different adducts of methylmalonate (MMA), propionate and propionyl-CoA (Pro-CoA) are the ones most accumulated in the samples from KO cells (Figure 3C and D, Table S3 and S4). MMA is the hydrolyzed form of methylmalonyl-CoA (M-CoA), the direct substrate of the mitochondrial B_{12} -dependent enzyme MUT, and propionate is the hydrolyzed form of Pro-CoA, the precursor of M-CoA (Figure 3E). It is notable that these are the same metabolites that accumulate in humans with B_{12} deficiency, and in fact, MMA is often used clinically as a marker of B_{12} deficiency. We detected metabolite ions that include $[M\text{-}H]^-$ and $[M\text{-}H\text{-}CO_2]^-$ adducts of MMA, and $[M\text{-}H]^-$ and $[M\text{-}2H]^{2-}$adducts of Pro-CoA in the cellular extract; $[M\text{-}H]^-$, $[M\text{-}H\text{-}CO_2]^-$ and an unknown adducts of MMA and $[M\text{-}H]^-$ adduct of propionate in the spent media (Table S5). Another unknown metabolite ion was also accumulated in the KO cellular extract, but database search failed to reveal its identity (Figure 3C). In addition, Clybl KO cells do not significantly accumulate homocysteine (Figure S2G), the substrate of the cytosolic B_{12} dependent enzyme, suggesting a specific defect in the mitochondrial B_{12} pathway.

Importantly, when a highly concentrated cellular metabolite extract was analyzed by LC-MS, the B_{12} cofactor for MUT, coenzyme B_{12} (AdoCbl), was consistently detected and significantly reduced in Clybl KO cells compared to the WT cells (Figure 3F). This observation is consistent with human genetics studies that linked CLYBL loss to a low B_{12} level in circulation (Grarup et al., 2013), and importantly, demonstrates a cell autonomous loss of coenzyme B_{12} in the absence of Clybl. This is rather striking since genes previously associated with low circulating B_{12} levels are involved in its absorption or trafficking (Grarup et al., 2013). This observation explains the accumulation of MMA since MUT is B_{12} dependent. Indeed, the accumulation of MMA in the Clybl KO cellular extracts can be rescued by either supplementing medium with 500 nM vitamin B_{12} (cyanocobalamin) or re-expressing human CLYBL construct that is resistant to the CRISPR reagents (Figure 3G), providing unequivocal evidence that the MMA accumulation is indeed due to loss of B_{12} in the setting of CLYBL loss.

Collectively, the prominent accumulation of MMA and propionate and the reduction of coenzyme B_{12} level in the Clybl KO cells, underscore a specific defect in mitochondrial B_{12} metabolism. These results demonstrate that loss of Clybl leads to a cell autonomous defect in B_{12} levels and specifically, in mitochondrial coenzyme B_{12}.

Enzymatic activity of CLYBL is required for maintaining mitochondrial B_{12}

A pressing question is how the newly identified citramalyl-CoA lyase activity of CLYBL is related to the maintenance of the mitochondrial B_{12} pathway. We therefore sought to rescue Clybl KO cells either with the wild-type allele or the catalytically dead $CLYBL^{D320A}$ mutant. Human $CLYBL^{D320A}$-FLAG protein is expressed at a similar level as the wild type human CLYBL-FLAG and endogenous murine Clybl (Figure 4A). While wild-type CLYBL reversed the accumulation of MMA, the reduction of coenzyme B_{12} and the accumulation of citramalyl-CoA, the catalytically inactive mutant $CLYBL^{D320A}$ failed to rescue any of these defects in the KO cells (Figure 4B–D). We conclude that the enzymatic activity of CLYBL is therefore required for maintaining mitochondrial B_{12} function.

Itaconyl-CoA directly inactivates coenzyme B_{12} via MUT

How does the loss of citramalyl-CoA lyase activity in the C5 pathway lead to a loss of mitochondrial B_{12}-dependent MUT activity? These two pathways are not obviously linked. An important clue emerged when we challenged wild-type brown adipocytes with 2 mM itaconate. Strikingly, these cells also exhibited a similarly increased level of MMA (Figure 5A) and decreased levels of coenzyme B_{12} (Figure 5B), mimicking the defects in mitochondrial B_{12} metabolism observed in the Clybl KO cells (Figure 3D and 3F).

This observation led us to hypothesize that elevated levels of a toxic intermediate due to CLYBL LOF might be responsible for inhibiting MUT activity. Notably, the CoA forms of some of these dicarboxylates, like itaconyl-CoA, are structurally similar to ethylmalonyl-CoA, a previously reported competitive inhibitor of the B_{12}-dependent MUT enzyme (Taoka et al., 1994).

But why might B_{12} levels themselves be reduced? We hypothesized that a toxic CoA ester formed upon CLYBL loss, which mimics the MUT substrate inactivates coenzyme B_{12} during the catalytic turnover cycle. If this mechanism is correct, then knocking out MUT genetically should suppress B_{12} deficiency in the face of CLYBL loss. To test this hypothesis, we generated the Clybl/Mut double knockout brown adipocytes using CRISPR technology (Figure 5C) and measured coenzyme B_{12} and MMA levels. The Mut KO cells did not show reduced coenzyme B_{12} levels (Figure 5D) despite the dramatic accumulation of MMA (Figure 5E), indicating that coenzyme B_{12} synthesis per se is not perturbed. Importantly, the reduction of coenzyme B_{12} levels in the Clybl KO cells was suppressed by genetic ablation of Mut (Figure 5D), suggesting that cofactor inactivation in the Clybl KO cells does in fact occur via the MUT enzyme. These experiments demonstrate that the loss of B_{12} in the setting of CLYBL loss requires MUT activity.

To directly identify the acyl-CoA inhibitor of MUT, we synthesized structurally related CoA esters in the C5 pathway (methylsuccinyl-CoA, mesaconyl-CoA, itaconyl-CoA and citramalyl-CoA), as well as the MUT substrate M-CoA, and tested their effects on recombinant human MUT reconstituted with coenzyme B_{12}. Strikingly, while all other CoA esters tested, including the M-CoA, did not affect the coenzyme B_{12} absorption spectrum (Figure 5F), the addition of itaconyl-CoA led to the immediate conversion of coenzyme B_{12} (λ_{max} = 529 nm) into cob(II)alamin (λ_{max} = 466 nm) (Figure 5G). Although cob(II)alamin

coupled to an organic radical is an intermediate in the MUT catalytic cycle, it is paramagnetic and susceptible to oxidative inactivation (Padovani and Banerjee, 2009). Hence, the unexpected stabilization of cob(II)alamin by itaconyl-CoA (versus coenzyme B_{12} by the natural substrate, M-CoA), increases the susceptibility of MUT to inactivation. The most parsimonious explanation of our results is that itaconyl-CoA accumulates in the setting of CLYBL loss, serves as suicide inhibitor for MUT and in the process, inactivates coenzyme B_{12}.

The immunomodulatory metabolite itaconate poisons B_{12} in many cell types

Itaconate is a recently identified anti-microbial and immunomodulatory metabolite in human, and is produced in millimolar quantities by activated macrophages (Jha et al., 2015; Michelucci et al., 2013; Strelko et al., 2011). The unexpected yet striking B_{12}-poisoning effect by the CoA ester of itaconate led us to determine if the same B_{12} inhibition mechanism of itaconyl-CoA extends to other cell types.

Itaconate added to HEK293T and human B-lymphocytes is converted to itaconyl-CoA inside cells and dramatically lowered the coenzyme B_{12} (Figure 6A and B). More strikingly, itaconate endogenously produced in activated macrophages is sufficient to inhibit coenzyme B_{12}. A 6-h LPS stimulation of murine macrophages dramatically increases itaconyl-CoA levels and completely ablates coenzyme B_{12} to undetectable levels (Figure 6C). Collectively, these experiments demonstrate that the CoA ester of itaconate is indeed a potent coenzyme B_{12} poison across different cell types, revealing an unexpected action of this immune metabolite.

Discussion

Recent genome-sequencing efforts have revealed that a small number of genes harbor bi-allelic, loss of function mutations in seemingly healthy humans (MacArthur et al., 2012). *CLYBL* is one such gene and ordinarily encodes a ubiquitously expressed mitochondrial enzyme of hitherto unknown function. The LoF polymorphism has been linked to reduced circulating B_{12} levels by GWAS studies (Grarup et al., 2013; Lim et al., 2014; Lin et al., 2012). To date, the precise enzymatic function of CLYBL and its link to B_{12} have remained obscure.

By combining genome editing, metabolomics, structural enzymology, we report that CLYBL functions as a citramalyl-CoA lyase and operates in the human C5 dicarboxylate pathway to detoxify itaconyl-CoA (Figure 7). In the absence of CLYBL, toxic CoA intermediates can serve as substrate analogs that deplete coenzyme B_{12} levels via a MUT-dependent mechanism. As a consequence, MMA and other upstream metabolites accumulate in cells with high MUT activity as well as an active C5 dicarboxylate pathway, such as the brown fat cells we used in the study. Through our study on CLYBL, we unexpectedly revealed a B_{12}-poisoning effect of itaconate, a recently identified immunometabolite. We further demonstrate that the same B_{12} inhibition effect of both exogenous and endogenous itaconate in various cell types, providing an unexpected connection between immunity and vitamin B_{12} metabolism.

Our work reveals a brand new endogenous inhibition mechanism of the mitochondrial B_{12}-dependent enzyme MUT that leads to rapid degradation of coenzyme B_{12}. MUT is a radical enzyme that utilizes substrate binding energy to trigger the homolytic cleavage of the Co-carbon bond in coenzyme B_{12}, and then propagates the carbon-based radical derived from AdoCbl to the substrate, facilitating a high-energy carbon skeleton rearrangement reaction. Coenzyme B_{12} is regenerated at the end of each reaction cycle (Banerjee and Ragsdale, 2003). Crystal structures of MUT reveal that the substrate fits snugly in a narrow corridor lined with conserved residues and that radical trajectories are controlled to avoid their extinction, which would lead to enzyme inhibition (Banerjee and Ragsdale, 2003; Padovani and Banerjee, 2006a). To our knowledge, itaconyl-CoA is the first reported substrate analogue that rapidly inactivates the B_{12} cofactor in the MUT enzyme. Previously, substrate analogs were found to inactivate MUT inefficiently (Taoka et al., 1994) or destroy coenzyme B_{12} when active site residues in MUT were mutated (Padovani and Banerjee, 2006a; Vlasie and Banerjee, 2004). While we detected citramalyl-CoA in cells lacking CLYBL, we did not observe itaconyl-CoA possibly because some of this toxic intermediate becomes covalently attached to the MUT enzyme during inactivation. While this hypothesis remains to be tested and the detailed mechanism will be elucidated in future studies, our observations provide a compelling mechanism for how CLYBL deficiency and itaconate exposure could lead to a B_{12} lowering effect.

We find that CLYBL participates in a relatively unexplored human C5 metabolic pathway. Studies in the 1960's reported that methylsuccinate, mesaconate and itaconate can be metabolized in the mouse liver (Adler et al., 1957; Montgomery et al., 1983; Wang et al., 1961). The first reaction involves conversion of these molecules into their corresponding CoA esters by the succinyl-CoA ligase complex. The second reaction, i.e., the hydration of mesaconyl-CoA and itaconyl-CoA into citramalyl-CoA is carried out by the promiscuous activity of AUH (methylglutaconyl-CoA hydratase). The third and final reaction requires a citramalyl-CoA lyase activity that had not been associated with any known enzyme (Wang et al., 1961). Here, we assign CLYBL to the missing citramalyl-CoA lyase activity, completing the elucidation of this C5 metabolic pathway. Although our experiments clearly establish a connection between itaconate, itaconyl-CoA and citramalyl-CoA, it is important to recognize that there are other sources of these toxic CoA esters in the cell. IRG1, the only mammalian enzyme currently known to produce itaconate, is expressed exclusively in activated macrophages (Jha et al., 2015; Michelucci et al., 2013; Strelko et al., 2011). In fact, in Clybl KO murine brown fat cells used in the study, we did not detect a high level of itaconate from the cell extract. Citramalyl-CoA is an intermediate in the catabolism of other C5 dicarboxylic acids including mesaconate and methylsuccinate, with the latter linked to isoleucine metabolism albeit via an unknown mechanism (Nowaczyk et al., 1998). Future studies will be required to define all the metabolic routes that are capable of generating citramalyl-CoA, and their relative contributions in different cell types.

Itaconate is a metabolite of growing interest in the context of innate immunity. Upon immune activation, itaconate is produced from macrophages at millimolar concentrations from the TCA cycle intermediate *cis*-aconitate, by *cis*-aconitate decarboxylase IRG1 (Jha et al., 2015; Michelucci et al., 2013; Strelko et al., 2011). Itaconate is reported to have anti-microbial activity, as it inhibits bacterial isocitrate lyase in the glyoxylate shunt, a pathway

not found in humans (McFadden and Purohit, 1977; Patel and McFadden, 1978; Williams et al., 1971). More recently, itaconate has been described as an anti-inflammatory metabolite whose activity is mediated in part by its ability to inhibit SDH and prevent ROS generation (Cordes et al., 2016; Lampropoulou et al., 2016; Luan and Medzhitov, 2016). Little is known about the fate of itaconate after immune activation. Our study proposes one of the routes for its metabolism into itaconyl-CoA and citramalyl-CoA, and finally pyruvate and acetyl-CoA via CLYBL. Future studies will be required to determine the relative contribution of this and other catabolic pathways in macrophages as well as in other cell types.

Our work reveals an unanticipated consequence of exposure to itaconate: B_{12} inactivation (Figure 7). Our experiments with macrophage demonstrates that endogenously produced itaconate during activation is sufficient to ablate coenzyme B_{12} in cell culture. We predict that *in vivo*, high concentrations of macrophage-derived itaconate might have autocrine and paracrine effects and poison B_{12} in nearby tissues, raising the possibility for a localized vitamin deficiency in the setting of inflammation. Itaconate is believed to serve as an antimicrobial metabolite by inhibiting the pathogen's glyoxylate shunt. In the future, it will be of interest to examine whether B_{12}-poisoning by itaconate also targets the bacterial homologs of MUT. If correct, this hypothesis will provide new insights into the antimicrobial function of itaconate, in addition to its known inhibition of isocitrate lyase. Future studies will need to assess whether the B_{12} inactivation mechanism contributes to the anti-microbial or anti-inflammatory effects of itaconate, and whether CLYBL regulates itaconate levels during immune activation. If the latter is true, then pharmacologically targeting CLYBL could have therapeutic value as an immunomodulator, especially since its inhibition is evidently well tolerated in humans.

An important future challenge lies in understanding why the premature stop polymorphism in *CLYBL* arose in the human population. To our knowledge, CLYBL is found as an intact gene in the genomes of all mammals, including non-human primates and ancient Neanderthals and Denisovans. Across humans, the stop polymorphism is extremely rare in Africans, and more common (MAF ~3–6%) in Northern Europeans, East Asians, and Ashkenazi Jews (Lek et al., 2016). One hypothesis is that *CLYBL* is becoming pseudogenized, perhaps because of changes in diet and nutrition, which obviate its need. Another possibility is simple genetic drift. A tantalizing alternative hypothesis is that, during human history, *CLYBL* loss may have conferred a selective advantage. If so, is this selection associated with CLYBL's role in vitamin B_{12} or itaconate metabolism in immunity? We anticipate that in the future, "reverse genomics" studies, which begin with human CLYBL knockouts, followed by in-depth clinical phenotyping, will be required to fully decipher the metabolic and immune consequences of loss of *CLYBL*, as well as its population genetic basis.

STAR Methods

Contact for Reagent and Resource Sharing

Further information and requests for resources and reagents should be directed to and will be fulfilled by the Lead Contact, Vamsi K. Mootha (vamsi@hms.harvard.edu).

Experimental Model and Subject Details

Cell Culture—Murine brown preadipocytes were a generous gift from the Bruce Spiegelman laboratory, and were previously reported (Pan et al., 2009). The HEK-293T cell line has the following STR profile: TH01 (7, 9.3); D21S11 (28, 29, 30.2); D5S818 (7,8,9); D13S317 (11,12,13,14,15); D7S820 (11); D16S539 (9, 13); CSF1PO (11,12,13); Amelogenin (X); vWA (16,18,19,20); TPOX (11). This profile matches 100% to HEK-293T cell line profile (ATCC, CRL-3216) if the Alternative Master's algorithm is used, and 83% if the Tanabe algorithm is used. RAW 264.7 cells (TIB-71) were obtained from ATCC, and B-lymphocytes (HG01971) were from Coriell Cell Repository. HEK-293T, RAW 264.7 cells and preadipocytes were cultured in DMEM supplemented with 10 % FBS, penicillin and streptomycin (both at 100 U/ml) under 5% CO_2 at 37 °C. B-lymphocytes were cultured in RPMI 1640 supplemented with 15 % FBS, penicillin and streptomycin (both at 100 U/ml) under 5% CO_2 at 37 °C. All cells were tested for mycoplasma contamination quarterly.

Lentivirus production using HEK-293T cells was described previously (Sancak et al., 2013). Briefly, preadipocytes were infected with the lentivirus for 2 days for stable expression of FLAG tagged proteins or for CRISPR knock out of endogenous genes, and selected for 2 days post-infection with 2 μg/ml puromycin or 200 μg/ml hygromycin. Lentivirus-infected preadipocytes were sub-cultured for 8 – 20 days before differentiation. Knockout efficiency was verified by western blot.

Brown adipocyte differentiation was performed according to a standard protocol. Briefly, preadipocytes were grown to confluence on day 0 before changing to differentiation medium (DMEM culture medium supplemented with 20 nM insulin and 1 nM T3). On Day 1, differentiation was induced by treating confluent cells for 2 days in the induction media (differentiation medium supplemented with 0.5 mM IBMX, 0.5 μM dexamethasone, and 0.125 mM indomethacin). Medium was changed to differentiation medium on day 3 and 5. All experiments with the differentiated brown adipocytes were performed after differentiation, between differentiation days 6 – 9, unless otherwise indicated.

For the rescue experiment, differentiated Clybl KO brown adipocytes were cultured in a DMEM-based medium supplemented with 500 nM cyanocobalamin (CNCbl) for 3 day before assay.

For CRISPR knockout, two sgRNAs per gene were cloned into pLentiCRISPRv2 plasmid (Addgene 52961) (Sanjana et al., 2014). A lentiviral pool from two guides was used for infection to achieve higher knockout efficiency. The sequences of the sgRNAs used are listed below:

Negative control	GCACTACCAGAGCTAACTCA
CLYBL sg1	GCGGAACACGGTTCGTGGAG
CLYBLsg6	CATAGAGCACTGCTCTCCGG
MUT sg1	CCGCACTGCAATCGAAGCCA
MUT sg3	TAAGTGACCACCCCGATGTC

Method Details

Oil Red O staining—Oil Red O staining was performed according to the protocol by Lonza. Briefly, Oil Red O stock solution was prepared by dissolving 300 mg Oil Red O in 100mL 99% isopropanol. Oil Red O working solution was prepared by mixing 3 parts Oil Red O stock solution with 2 parts deionized water. This mixture was allowed to sit at room temperature for 10 min before being filtered to remove particles. Oil Red O working solution was used within 2 hours of preparation.

Differentiated brown adipocytes were rinsed with sterile PBS solution, fixed for 30–60 min at room temperature in 10% neutral buffered formalin, rinsed with sterile water, and washed with 60% isopropanol for 2–5 min before staining in Oil Red O working solution for 5 minutes. The cells were then carefully rinsed with water to remove excess Oil Red O and stored in water.

Quantitative PCR to measure relative RNA levels—RNA was extracted from cells using the QIAGEN RNeasy Mini kit according to the manufacturer's instructions. The cDNA was prepared from template RNA using the Superscript III First-Strand Synthesis Kit for qRT-PCR.

All qRT-PCR reactions were conducted on a 7500 Fast Real-Time PCR System (Applied Biosystems) using TaqMan reagents. For each reaction, 10 μl of TaqMan Fast Master Mix was mixed with 9 μl of cDNA and 1 μl of the appropriate TaqMan probe. The cDNA was amplified using the pre-programmed fast ramp speed protocol. Data was analyzed using the $\Delta\Delta C_T$ method, using HPRT as a housekeeping gene for normalization.

Measurement of cellular oxygen consumption rate—Oxygen consumption rates were measured using a Seahorse XF24 Extracellular Flux Analyzer (Seahorse Bioscience). Preadipocytes were seeded in Seahorse XF24 24-well cell culture microplates and differentiated in wells using the protocol mentioned above. On differentiation day 6, the cell culture media was replaced with 500 μl DMEM with low glucose/L-glutamine/no sodium pyruvate, supplemented with 25 mM HEPES-KOH, pH 7.4. Oxygen consumption was then measured on differentiation day 7. Each measurement was performed over 4 min after a 2-min mix and a 2-min wait period.

CLYBL plasmids—Bacteria codon-optimized construct coding a C-terminal Hisx6-tagged human CLYBL lacking the mitochondrial targeting sequence (aa 23–340) was custom synthesized and subcloned into pET30a vector by GENEWIZ. A C-terminal Hisx6-tagged human $CLYBL^{D320N}$ plasmid was prepared by site-directed mutagenesis kit (QuikChange Lightning, Agilent).

A C-terminal FLAG-tagged human CLYBL construct was generated as following: DNA sequence coding full-length human CLYBL without the stop codon was custom synthesized by GENEWIZ and subcloned in gateway pDONR223. The CLYBL DNA was further amplified by PCR and subcloned into an in-house lentiviral expression vector (Plys1 vector) bearing a C-terminal FLAG tag using Nhe1 – AgeI/XmaI sites.

The sequence of the CLYBL-coding region is:

ATGGCGCTACGTCTGCTGCGGAGGGCGGCGCGCGGAGCTGCGGCGGCGGCGCTGCTGAGGC

TGAAAGCGTCTCTAGCAGCTGATATCCCCAGACTTGGATATAGTTCCTCATCCCATCACAAG

TACATCCCCCGGAGGGCAGTGCTATACGTTCCAGGAAATGATGAAAAGAAAATAAAGAAGA

TTCCATCCCTGAATGTAGATTGTGCAGTGCTCGACTGTGAGGATGGAGTGGCTGCAAACAAA

AAGAATGAAGCTCGACTGAGAATTGTAAAAACTCTTGAAGACATTGATCTGGGCCCTACTGA

AAAATGTGTGAGAGTCAACTCAGTTTCCAGTGGTCTGGCGGAAGAAGACCTAGAGACCCTTT

TGCAATCCCGGGTCCTTCCTTCCAGCCTGATGCTACCAAAGGTGGAAAGTCCTGAAGAAATC

CAGTGGTTTGCAGACAAATTTTCATTCCACTTAAAAGGCCGAAAACTTGAACAACCAATGAA

TTTAATCCCTTTTGTGGAAACTGCAATGGGTTTGCTCAATTTTAAGGCAGTGTGTGAAGAAAC

CCTGAAGGTCGGGCCTCAAGTAGGTCTCTTTCTAGATGCAGTCGTTTTTGGAGGAGAAGACT

TTCGAGCCAGCATAGGGGCCACGTCGAGTAAAGAAACCCTGGATATTCTCTACGCCCGGCAA

AAGATTGTTGTCATAGCGAAAGCCTTTGGTCTCCAAGCCATAGATCTGGTGTACATTGACTTT

CGAGATGGAGCTGGGCTGCTTAGACAGTCACGAGAAGGAGCCGCCATGGGCTTCACTGGTA

AGCAGGTGATTCACCCTAACCAAATTGCCGTGGTCCAGGAGCAGTTTTCTCCTTCCCCTGAA

AAAATTAAGTGGGCTGAAGAACTGATTGCTGCCTTTAAAGAACATCAACAATTAGGAAAGG

GGGCCTTTACTTTCCAAGGGAGTATGATCGAC

ATGCCATTACTGAAGCAGGCCCAGAACACTGTTACGCTTGCCACCTCCATCAAGGAAAAA

The C-terminal FLAG-tagged human CLYBL^{D320A} and CLYBL^{D320A} plasmids were prepared from CLYBL plasmid in pDONR223 vector by site-directed mutagenesis kit (QuikChange Lightning, Agilent), and then subcloned into the Plys1 vector.

Expression and purification of recombinant human CLYBL—Expression and purification of CLYBL was performed with standard procedures. Briefly, *E.coli* BL21 (DE3) cells transformed with the wild type or mutant CLYBL plasmid were grown in 1 L terrific broth supplemented with 50 μg/ml kanamycin. After induction with 0.25 mM IPTG, the flask were incubated at 15 °C overnight. Cell pellets were suspended and sonicated in 500 ml lysis buffer (20 mM Tris pH 8, 500 mM NaCl, 10 % glycerol, 10 mM $MgCl_2$, 5 mM imidazole and 1 mM TCEP) containing 5 μl benzonase and protease inhibitor cocktail tablets. His-tagged fusion proteins were affinity purified using TALON cobalt resin followed by size-exclusion chromatography in buffer containing 20 mM Tris pH 8, 150 mM NaCl, 10 mM $MgCl_2$ and 1 mM TCEP.

CoA esters synthesis—Malyl-CoA and methylmalyl-CoA were synthesized enzymatically with recombinant (*S*)-malyl-CoA/β-methylmalyl-CoA/(*S*)-citramalyl-CoA lyase from *C. aurantiacus* (CaMCLC) (Zarzycki et al., 2009). Citramalyl-CoA ((*S*)-form throughout the paper) was synthesized enzymatically with either CaMCLC or *P.aeruginosa* succinyl-CoA:itaconate CoA transferase (PaIct) (Sasikaran et al., 2014). Itaconyl-CoA was synthesized enzymatically using Palct (Sasikaran et al., 2014). Methylsuccinyl-CoA and mesaconyl-CoA were chemically synthesized by Acme Bioscience (Palo Alto, CA).

For the recombinant enzymes, bacteria codon-optimized, C-terminal His-tagged CaMCLC plasmid was custom synthesized and subcloned into pET21a vector by GenScript; bacteria codon-optimized, N-terminal His-tagged paIct plasmid was custom synthesized and subcloned into pET30a vector by GENEWIZ. Recombinant protein expression was performed similarly with human CLYBL. Specifically, bacteria were lysed in a similar lysis buffer for human CLYBL but supplemented with an additional 20 % (v/v) bug buster protein extraction reagent. Proteins were affinity purified using TALON cobalt resin. CaMCLC was further purified by size exclusion chromatography. The enzymatic activities of protein batches were tested before the assay.

For CoA esters synthesis using CaMCLC, Malyl-CoA was synthesized from glyoxylate and acetyl-CoA, methylmalyl-CoA from glyoxlyate and propionyl-CoA, and citramalyl-CoA from pyruvate and acetyl-CoA. Specifically, a 500 μl reaction mixture containing 100 mM MOPS pH 7.5, 5 mM $MgCl_2$, 1 mM TCEP, 50 mM glyoxylate or pyruvate, 10 mM acetyl-CoA or propionyl-CoA and 20 μg CaMCLC enzyme were incubated at 45 °C for 20 min. The reaction was quenched by adding 5 μl formic acid and the synthesized CoA esters was purified using HPLC method.

For CoA esters synthesis using PaIct, itaconyl-CoA was synthesized from itaconate and succinyl-CoA, and citramalyl-CoA was from citramalate and succinyl-CoA. Specifically, a 500 μl reaction mixture containing 100 mM MOPS pH 7.5, 5 mM $MgCl_2$, 1 mM TCEP, 100 mM itaconate or citramalate, 10 mM succinyl-CoA and 250 μg Palct enzyme were incubated at 37 °C for 10 min. The reaction was quenched by adding 5 μl formic acid and the synthesized CoA esters were purified using HPLC method.

The purity of the CoA esters is estimated by HPLC. CoA esters synthesized by CaMCLC are > 80% pure, itaconyl-CoA synthesized by PaIct is 80% pure, and citramalyl-CoA is 60%

pure. Chemically synthesized methylsuccinyl-CoA is 30% pure and mesaconyl-CoA is 100% pure with a mixture of C1 and C4 CoA form.

CoASH and CoA ester quantification and purification by HPLC—Agilent 1260 HPLC system with a reversed-phase C_{18} column (Luna 5μm C18 100 Å 150 × 4.6 mm, Cat. # 00F-4041-E0, phenomenex) was used for CoA and CoA esters quantification. The mobile phase A was 40 mM ammonium formate/formic acid pH 4. The mobile phase B was 100% acetonitrile. The flow rate was 0.8 ml/min. A 20-min gradient elution was as follows: 0 min: 2% B; 2 min: 2% B; 10 min: 15% B; 12 min: 50% B; 15 min: 50% B; 17 min: 2% B. CoASH and CoA esters were detected by UV absorbance at 260 nm. The amount of CoA esters was calculated from the relative peak area. The identification of the CoA esters was based on co-chromatography with standards and accurate mass by LC-MS. Retention times were: CoASH, 10.0 min; citramalyl-CoA 10.5 min; acetyl-CoA, 11.5 min; propionyl-CoA 13.8 min; methylmalyl-CoA, 10.5 min; malyl-CoA, 9.5 min; and itaconyl-CoA 12 min.

The absolute concentration of the CoA esters was measured by UV-visible spectra on a Cary 100 spectrophotometer (Agilent, CA). An extinction coefficient (CoA, 260 nm) = 16.4 $mM^{-1}.cm^{-1}$ was used to calculate the concentration of the CoA esters.

Enzyme Assay—All discontinuous enzyme assays for CLYBL were performed by HPLC method measuring CoASH and CoA esters.

Malate/citramalate/methylmalate/dimethylmalate synthase activity: For the forward reaction activity, the formation of free CoASH was monitored. A 200 μl reaction mixture containing 20 mM Tris pH7.5, 5 mM $MgCl_2$, 1mM TCEP, 20 mM glyoxylate or pyruvate, different concentration (2.5 – 200 μM) of propionyl-CoA or acetyl-CoA and purified human CLYBL protein (2 μg for malate/methylmalate synthase activity and 4 μg for citramalate synthase activity) were incubated at 37 °C for 3 and 6 min (for malate/methylmalate synthase activity) and for 3 and 7 min (for citramalate synthase activity). At each time point, a 70 μl reaction mixture was taken and immediately quenched by adding 5 μl formic acid. A 20 μl quenched reaction mixture was injected for HPLC analysis and quantified for the enzyme parameter.

Citramalyl-CoA lyase activity: For the reverse reaction activity (malyl-CoA/citramalyl-CoA/methylmalyl-CoA lyase), the formation of acetyl-CoA or propionyl-CoA was monitored. Only citramalyl-CoA lyase activity was detected, while malyl-CoA or methylmalyl-CoA lyase activities were not detected. A malyl-CoA esterase activity was also detected but not quantified. For the citramalyl-CoA lyase activity, a 300 μl reaction mixture containing 20 mM Tris pH7.5, 5 mM $MgCl_2$, 1mM TCEP, different concentration (0.625 – 80 μM) of citramalyl-CoA and 10 ng purified human CLYBL protein were incubated at 37 °C for 2 and 5 min. At each time point, a 100 μl reaction mixture were taken and immediately quenched by adding 10 μl formic acid. A 90 μl quenched reaction mixture were injected for HPLC analysis and quantified to determine the enzyme activity.

Human CLYBL crystallization and structure determination—Crystals of wild type human CLYBL were grown by sitting drop vapor diffusion method in the screen and

hanging drop vapor diffusion method during the optimization. The initial crystallization screen was performed with MCSG suite (Microlytic, MA) using the NanoTransfer NT8 pipetting robot (Formulatrix, MA) and the crystals were monitored daily with Rock Maker (Formulatrix, MA).

For the apo form, 1 μl of human CLYBL protein at 4 mg/ml in 20 mM Tris pH 8, 150 mM NaCl, 10 mM $MgCl_2$ and 1 mM TCEP was mixed with 1 μl well solution containing 85 % of the following solution diluted in water: 0.2 M ammonium citrate dibasic (pH 4.5 – 5.5), 20% (w/v) PEG 3350. For the complex-PEG form, 1 μl of human CLYBL protein at 4 mg/ml in 20 mM Tris pH 8, 150 mM NaCl, 10 mM $MgCl_2$ and 1 mM TCEP also containing 5 mM propionyl-CoA and 10 mM glyoxylate was mixed with 1 μl well solution: 0.1 M Na_2HPO_4:citric acid pH 4.2, 40% (v/v) PEG 300. As citrate sequestered the magnesium, the magnesium ion in the active site of CLYBL in the apo form and the complex-PEG form is absent. Propionyl-CoA molecules were bound at the substrate binding pockets. For the complex-formate form, 1 μl of human CLYBL protein at 4 mg/ml in 20 mM Tris pH8, 150 mM NaCl, 10 mM $MgCl_2$ and 1 mM TCEP also containing 5 mM propionyl-CoA and 10 mM glyoxylate was mixed with 1 μl well solution: 0.1 M sodium acetate:HCl pH 4.6, 3.5 M sodium formate. In the complex-formate form, free CoASH molecules were seen in the substrate binding pockets due to CLYBL catalysis. In all three conditions, the crystals were transferred to the well solution containing an additional 20% ethylene glycol and flash cooled in liquid nitrogen.

X-ray diffraction data were collected at beamline 8.2.2 at the Advanced Light Source (Berkeley, CA). Data collected at λ = 0.99997 Å with 3×3 CCD array (ADSC Q315R) detector were indexed, integrated and scaled using the software autoPROC (Global Phasing, Ltd.) software (Vonrhein et al., 2011), in which CC1/2 and I /σ were used as the criteria for high resolution shells (Diederichs and Karplus, 2013; Karplus and Diederichs, 2012, 2015). The structure of complex-formate form was solved by molecular replacement using Phaser software (McCoy et al., 2007), with the structure of *M. tuberculosis* citE (PDB accession number 1z6k) as a search model. The structures of complex-PEG and apo form were solved by molecular replacement using the complex-formate structure as a search model. The final model was built in the Coot molecular graphics application (Emsley et al., 2010) and refined with Phenix (Adams et al., 2010) and Buster (Global Phasing, Ltd.) software (Bricogne et al., 2016). All data collection and refinement statistics are summarized in Table S2. All protein structure figures were generated using PyMOL program (The PyMOL Molecular Graphics System, Version 1.7.x. Schrödinger, LLC.).

Structure docking of citramalyl-CoA—The structure docking was performed using Schrödinger Suite 16 software. For preparing the complex CLYBL protein structure, all the coordinates were from the complex-formate structure, except one propionyl-CoA, which was from a superimposed CLYBL trimer in the complex-PEG form and was retained for the positioning purpose. Addition of hydrogen atoms, assignment atomic charges, elimination water beyond 5 Å from the proteins and ligands were generated by Protein Preparation Wizard application (Sastry et al., 2013). RMSD convergence criterion was set as 0.30Å to minimize the structural hydrogen and the whole structure was refined in the OPLS force field. Ligand citramalyl-CoA was prepared using LigPrep application and two low energy

ring conformations at pH 7.4 with the OPLS force field were selected. Docking calculations were performed using Glide docking application following the Induced Fit Docking (IFD) protocol (Farid et al., 2006).

***In vitro* activity based metabolite profiling—**Adult male mice were starved overnight before anesthetization in a CO_2 chamber. Mouse livers were immediately frozen in liquid nitrogen, lyophilized for 2 hours, and ground to powder using bioPulverizer prior chilled in liquid nitrogen. Approx. 2 g frozen tissue powder was subject to a two-step extraction. The first extraction was performed by adding 500 μl ice-cold 50% methanol containing 20 mM ammonium formate and formic acid at pH 4, and 375 μl chloroform. The mixture was vortexed for 15 sec before centrifugation at 13,200 rpm for 10 min at 4 °C. After transferring the top layer to another 2 ml eppendorf tube, the bottom layer was extracted again by adding 500 μl ice-cold H_2O/methanol/acetonitrile (45:50:5 vol/vol/vol) and centrifugation at 13,200 rpm for 10 min at 4 °C. The two top layers were combined, dried using SpeedVac with the low-temperature setting for 1 hour and then lyophilized overnight. The dried metabolite mixture was suspended in 1 ml ice-cold 20 mM Tris pH7.5 buffer, sonicated in a water batch sonicator for 10 min at room temperature, and centrifuged at 13,200 rpm for 10 min at 4 °C. The resulting supernatant was aliquoted and stored at −80 °C.

For each reaction, a 25 μl tissue metabolite extract was mixed with 6 μg recombinant human CLYBL or $CLYBL^{D320N}$ in an eppendorf tube and the mixture was incubated at 37 °C for 0, 10, 30 or 60 min. Each condition was repeated in triplicate. At the end of the incubation, the reaction was quenched and the metabolites extracted by adding 70 μl ice-cold LC-MS grade acetonitrile, centrifuged at 13,200 rpm for 10 min at 4 °C, and the supernatant were transferred into a LC-MS glass vial for LC-MS analysis.

LC-MS based metabolite profiling and metabolomics—LC/MS-based analyses were performed on a Q Exactive benchtop orbitrap mass spectrometer equipped with an Ion Max source and a HESI II probe, which was coupled to a Dionex UltiMate 3000 UPLC system (Thermo Fisher Scientific).

HILIC negative method for polar metabolites

Cellular metabolomics: Clybl KO and control brown adipocytes were differentiated in 6 well plates. Medium was changed to fresh DMEM culture medium 24 hours, one hour before and changed again for the assay. Metabolites from 3 day spent media and cellular metabolites were extracted for analysis.

For spent media metabolites, 50 μl spent media sample was aliquoted in the Eppendorf tube and mixed with 450 μl ice-cold acetonitrile:methanol (75:25 vol/vol). For cellular metabolites, cells were washed with 2 ml ice-cold 100 mM ammonium acetate pH 7.5 twice, scraped in 500 μl ice-cold extraction buffer acetonitrile:methanol:H_2O (67.5:22.5:10 vol/vol/vol) and transferred to the Eppendorf tube. The extraction mixture was vortexed and centrifuged at 13,200 rpm for 10 min at 4 °C, and a 100 μl supernatant was transferred into LC-MS glass vial for analysis.

Xbridge BEH Amide XP HILIC 2.5 μm, 2.1 mm × 100 mm column (Waters, 186006091) was used for analysis. The column was maintained at 27 °C during the analysis. The mobile phase A was 20 mM ammonium acetate/0.25% ammonium hydroxide pH 9.0. The mobile phase B was 100% acetonitrile. The flow rate was 220 μl/min. The gradient elution was as follows: 0 min: 85% B; 0.5 min: 85% B; 9 min: 35% B; 11 min: 2% B; 12 min: 85% B; 25 min: 85% B.

The MS data acquisition was collected in the negative polarity with full scan mode in a range of 70–1000 m/z, with the spray voltage set to 2.5 kV, the heated capillary at 310 °C, the HESI probe held at 370 °C, the sheath gas flow set to 50 units, the auxiliary gas flow set to 10 units, the sweep gas flow set to 2 unit, the resolution set at 140,000, the AGC target at 3E6, and the maximum injection time at 400 ms. The injection order of samples was randomized. Progenesis QI software (Waters, NC) was used to perform peak picking, peak alignment, and peak intensity integration.

Metabolomics data analysis

Cellular metabolomics: After Progenesis QI peak intensity integration, two filters were applied: minimum abundance >2500, and max coefficient of variation within quadruplicate (stdev/mean) <0.8. 1582 features were included in the 3 day cellular metabolite profiling, and 1660 features in the 3 day spent media. The filtered metabolite lists were then annotated by searching against in-house chemical standard library with 5-ppm mass accuracy and 0.5-min retention time difference, and manual curation was performed. For cellular profiling, fold change > 5 and p-value > 0.05 are highlighted; for spent media, fold change > 2 and p-value > 0.05 are highlighted. For the highlighted metabolites, after the database search, the identities of the known metabolites were further confirmed by chemical standards.

In vitro activity-based metabolomics: After Progenesis QI peak intensity integration, two filters were applied: minimum abundance >1000, and max coefficient of variation within quadruplicate (stdev/mean) <0.8. 3011 features are included.

HILIC positive method for homocysteine measurement: Homocysteine is detected from the spent media samples. Specifically, a 200 μl spent media sample from the differentiated Clybl KO and control brown adipocytes was reduced by adding 20 μl 1 M DTT at room temperature for 15 min. After the incubation, a 60 μl supernatant was aliquoted in the Eppendorf tube and mixed with 120 μl ice-cold acetonitrile: methanol (75:25 vol/vol) supplemented with 0.1% formic acid. The mixture was vortexed and centrifuged at 13,200 rpm for 10 min at 4 °C, and 100 μl supernatant was transferred into LC-MS glass vial for analysis.

Atlantis HILIC Silica 3 μm, 2.1 mm × 150 mm column (Waters, 186002015) was used for analysis. The column was maintained at 27 °C during the analysis. The mobile phase A was 10 mM ammonium fomate/0.1% formic acid. The mobile phase B was 100% acetonitrile with 0.1% formic acid. The flow rate was 250 μl/min. The gradient elution was as follows: 0 min: 95% B; 0.5 min: 95% B; 10.5 min: 40% B; 15 min: 40% B; 17 min: 95% B; and 32 min 95% B.

The MS data acquisition was collected in the positive polarity with full scan mode in a range of 70–1000 m/z, with the spray voltage set to 2.5 kV, the heated capillary at 310 °C, the HESI probe held at 370 °C, the sheath gas flow set to 50 units, the auxiliary gas flow set to 10 units, the sweep gas flow set to 2 unit, the resolution set at 140,000, the AGC target at 3E6, and the maximum injection time at 400 ms. The relative intensities of homocysteine were quantified using Xcalibur QualBrowser or QuanBrowser software (Thermo Fischer Scientific) with mass tolerance of 5 ppm and 3 point smoothing. The identity of the homocysteine is confirmed by the chemical standard from the IROA Technologies library.

C18 SIM method for AdoCbl measurement: Cellular metabolites from brown adipocytes cultured in 6-well plates were extracted as previously mentioned, but kept in dark throughout the sample preparation. Metabolite extracts were lyophilized overnight, suspended in 60 μl 7.5% acetonitrile in 25 mM ammonium formate/formic acid pH4, centrifuged at 13,200 rpm for 10 min at 4 °C, and supernatant was transferred into LC-MS glass vial for analysis.

Acquity BEH C18 1.7 μm, 2.1 mm × 75 mm (Waters, 186002352) was used for analysis. The column was maintained at 27 °C during the analysis. The mobile phase A was 25 mM ammonium formate/formic acid pH 4. The mobile phase B was 100% acetonitrile. The flow rate was 250 μl/min. The gradient elution was as follows: 0 min: 7.5% B; 10 min: 22.5% B; 15 min: 50% B; 17 min: 50% B; 19 min: 25% B; 20 min: 7.5% B; 30 min: 7.5% B.

The MS data acquisition method was optimized with the chemical standard AdoCbl. Specifically, the data were collected in the positive polarity and targeted-SIM scans for AdoCbl ($[M+2H]^{2+}$ with 790.3365 m/z), with the spray voltage set to 4 kV, the heated capillary at 325 °C, the HESI probe held at 300 °C, the sheath gas flow set to 40 units, the auxiliary gas flow set to 10 units, the sweep gas flow set to 1 unit, the resolution set at 70,000, the AGC target at 5E5, the maximum injection time at 200 ms, and isolation window at 2.0 m/z.

The relative intensities of AdoCbl were quantified using Xcalibur QualBrowser or QuanBrowser software (Thermo Fischer Scientific) by measuring the area under the curve with mass tolerance of 5 ppm and 3 point smoothing.

C18 scan method for acyl-CoA measurement: Cellular acyl-CoAs extraction from brown adipocytes was performed similarly as the AdoCbl measurement, except that a 60 cm dish was used.

Acquity BEH C18 1.7 μm, 2.1 mm × 75 mm (Waters, 186002352) was used for the analysis. The column was maintained at 27 °C during runs. The mobile phase A was 25 mM ammonium formate/formic acid pH 4. The mobile phase B was 100% acetonitrile. The flow rate was 250 μl/min. The gradient elution was as follows: 0 min: 2 % B; 2 min: 2% B; 15 min: 50% B; 17 min: 98% B; 25 min: 98% B; 27 min: 2% B; 35 min: 2% B.

The MS data acquisition was collected in the positive polarity with full scan mode in a range of 300–1000 m/z, with the spray voltage set to 4 kV, the heated capillary at 325 °C, the HESI probe held at 300 °C, the sheath gas flow set to 40 units, the auxiliary gas flow set to

10 units, the sweep gas flow set to 1 unit, the resolution set at 70,000, the AGC target at 3E6, and the maximum injection time at 400 ms.

Data analysis was performed using Xcalibur QualBrowser or QuanBrowser software (Thermo Fischer Scientific) by measuring the area under the curve with mass tolerance of 5 ppm and 3 point smoothing. The identities of CoA esters were confirmed by CoA ester standards.

Itaconate-$^{13}C_5$ labeling experiment—Itaconate-$^{13}C_5$ was obtained from either NIH Common Fund Metabolite Standards Synthesis Core or from Santa Cruz Biotechnology (sc-495554). Wild type brown adipocytes were differentiated in 60 cm dish, and incubated with regular DMEM-based culture medium supplemented with 1 mM itaconate-$^{13}C_5$ or unlabeled itaconate for 3 days before metabolite extraction and LC-MS analysis.

Exogenous itaconate addition experiment—For brown adipocytes, differentiated wild type cells in 60 cm dishes were incubated with regular DMEM-based culture medium supplemented with 2 mM itaconate for 3 days before metabolite extraction and LC-MS analysis for CoA esters and coenzyme B_{12}. For HEK293T cells, 2 million cells were plated in 60 cm dishes overnight, medium was changed to DMEM-based culture medium supplemented with 2 mM itaconate for one day before the assay. For B-lymphocytes, 5 million cells were pelleted and suspended in 10 ml DMEM-based culture medium in T25 flasks; a final concentration of 2 mM itaconate was added to the culture for one day before the assay. The suspension cells were pelleted at 600 g for 5 min at 4 °C, washed once with 1 ml ice-cold PBS and once with 1 ml ice-cold 100 mM ammonium acetate pH 7.5 before extraction using the same protocol mentioned above.

Macrophage experiment—For RAW 264.7 macrophage experiments, 3.5 million cells were plated in 60 cm dishes in DMEM-based culture medium one day before the assay. The next day, the medium were changed to fresh DMEM-based culture medium with or without 10 ng/ml LPS and incubated for 6 hours before extraction and LC-MS analysis for B_{12} and CoA esters following the protocol described above.

MUT inhibition assay

Human MUT protein production: A human *mut* gene that was codon optimized for *E. coli* expression was synthesized by GenScript and cloned into a pET28b vector using NcoI and XhoI restriction enzymes. The recombinant protein was expressed and purified as described previously (Froese et al., 2010).

Methylmalonyl-CoA synthesis: Methylmalonyl-CoA was synthesized using malonyl-CoA synthetase and purified as described previously (Padovani and Banerjee, 2006b).

Inactivation of human MUT enzyme: Human MUT (35 μM monomer) in 50 mM Hepes pH 7.5 containing 150 mM KCl, 2 mM $MgCl_2$, 2 mM TCEP, and 5% glycerol was reconstituted by incubating with AdoCbl (30 μM) for 10 min at 30 °C. After recording the initial absorption spectrum, itaconyl-CoA or methylmalonyl-CoA were added to a final concentration of 600 μM. Spectra were recorded before and after addition of the acyl-CoAs.

Other acyl-CoAs (methylsuccinyl-CoA, mesaconyl-CoA, citramalyl-CoA) were also tested but failed to show evidence of inactivation even at a higher temperature.

Quantification and Statistical Analysis—All p values were calculated using unpaired two-tailed Student's t-test with Graphpad Prism software or Excel. No specific randomization or blinding protocol was used for these analyses. Error bars in figures indicate standard deviation (SD) for at least three replicates. All LC-MS experiments are performed in quadruplicates, and repeated at least three times.

Data and Software Availability—The atomic coordinates of the human CLYBL in apo form and the two complex forms are deposited to the Protein Data Bank under the accession code PDB: 5VXC, 5VXO and 5VXS, respectively.

Supplementary Material

Refer to Web version on PubMed Central for supplementary material.

Acknowledgments

We thank B. Spiegelman for providing the immortalized brown adipocyte cell line; L. Strittmatter, R. Sharma, and J. Peng for expert technical advice; S. Calvo and I. Jain for computational assistance; V. Cracan and members of Mootha lab for fruitful discussions and feedback. This research used resources of the Advanced Light Source, which is a DOE Office of Science User Facility under contract no. DE-AC02-05CH11231. We acknowledge the NIH Common Fund Metabolite Standards Synthesis Core for providing itaconate-$^{13}C_5$. This work was supported by NIH grants R24DK080261 and R35GM122455 (to V.K.M.), R01DK45776 (to R.B.), NSFC 21472208, 81625022, 81430084 and 21210003 (to C.L.), F32GM114905 and K99GM124296 (to H.S.), F32GM113405 (to G.C.) and F31DK107187 (to D.F.). V.K.M. is an Investigator of the Howard Hughes Medical Institute.

References

Adams PD, Afonine PV, Bunkoczi G, Chen VB, Davis IW, Echols N, Headd JJ, Hung LW, Kapral GJ, Grosse-Kunstleve RW, et al. PHENIX: a comprehensive Python-based system for macromolecular structure solution. Acta Crystallogr. D Biol. Crystallogr. 2010; 66:213–221. [PubMed: 20124702]

Adler J, Wang SF, Lardy HA. The metabolism of itaconic acid by liver mitochondria. J. Biol. Chem. 1957; 229:865–879. [PubMed: 13502348]

Banerjee R, Gherasim C, Padovani D. The tinker, tailor, soldier in intracellular B12 trafficking. Curr. Opin. Chem. Biol. 2009; 13:484–491. [PubMed: 19665918]

Banerjee R, Ragsdale SW. The many faces of vitamin B12: catalysis by cobalamin-dependent enzymes. Annu. Rev. Biochem. 2003; 72:209–247. [PubMed: 14527323]

Bracken CD, Neighbor AM, Lamlenn KK, Thomas GC, Schubert HL, Whitby FG, Howard BR. Crystal structures of a halophilic archaeal malate synthase from Haloferax volcanii and comparisons with isoforms A and G. BMC Struct. Biol. 2011; 11:23. [PubMed: 21569248]

Bricogne, G., Blanc, E., Brandl, M., Flensburg, C., Keller, P., Paciorek, W., Roversi, P., Sharff, A., Smart, OS., Vonrhein, C. version 2.10.1. Cambridge, United Kingdom: Global Phasing Ltd; 2016.

Calvo SE, Clauser KR, Mootha VK, et al. MitoCarta2.0: an updated inventory of mammalian mitochondrial proteins. Nucleic Acids Res. 2016; 44:D1251–1257. [PubMed: 26450961]

Cordes T, Wallace M, Michelucci A, Divakaruni AS, Sapcariu SC, Sousa C, Koseki H, Cabrales P, Murphy AN, Hiller K, et al. Immunoresponsive Gene 1 and Itaconate Inhibit Succinate Dehydrogenase to Modulate Intracellular Succinate Levels. J. Biol. Chem. 2016; 291:14274–14284. [PubMed: 27189937]

de Carvalho LP, Zhao H, Dickinson CE, Arango NM, Lima CD, Fischer SM, Ouerfelli O, Nathan C, Rhee KY. Activity-based metabolomic profiling of enzymatic function: identification of Rv1248c as

a mycobacterial 2-hydroxy-3-oxoadipate synthase. Chem. Biol. 2010; 17:323–332. [PubMed: 20416504]

Diederichs K, Karplus PA. Better models by discarding data? Acta Crystallogr. D Biol. Crystallogr. 2013; 69:1215–1222. [PubMed: 23793147]

Dimroth P, Eggerer H. Isolation of subunits of citrate lyase and characterization of their function in the enzyme complex. Proc. Natl. Acad. Sci. U. S. A. 1975; 72:3458–3462. [PubMed: 1060145]

Emsley P, Lohkamp B, Scott WG, Cowtan K. Features and development of Coot. Acta Crystallogr..z D Biol. Crystallogr. 2010; 66:486–501.

Farid R, Day T, Friesner RA, Pearlstein RA. New insights about HERG blockade obtained from protein modeling, potential energy mapping, and docking studies. Bioorg. Med. Chem. 2006; 14:3160–3173. [PubMed: 16413785]

Froese DS, Kochan G, Muniz JR, Wu X, Gileadi C, Ugochukwu E, Krysztofinska E, Gravel RA, Oppermann U, Yue WW. Structures of the human GTPase MMAA and vitamin B12-dependent methylmalonyl-CoA mutase and insight into their complex formation. J. Biol. Chem. 2010; 285:38204–38213. [PubMed: 20876572]

Gherasim C, Lofgren M, Banerjee R. Navigating the B(12) road: assimilation, delivery, and disorders of cobalamin. J. Biol. Chem. 2013; 288:13186–13193. [PubMed: 23539619]

Grarup N, Sulem P, Sandholt CH, Thorleifsson G, Ahluwalia TS, Steinthorsdottir V, Bjarnason H, Gudbjartsson DF, Magnusson OT, Sparso T, et al. Genetic architecture of vitamin B12 and folate levels uncovered applying deeply sequenced large datasets. PLoS Genet. 2013; 9:e1003530. [PubMed: 23754956]

Harper AR, Nayee S, Topol EJ. Protective alleles and modifier variants in human health and disease. Nat. Rev. Genet. 2015; 16:689–701. [PubMed: 26503796]

Jha AK, Huang SC, Sergushichev A, Lampropoulou V, Ivanova Y, Loginicheva E, Chmielewski K, Stewart KM, Ashall J, Everts B, et al. Network integration of parallel metabolic and transcriptional data reveals metabolic modules that regulate macrophage polarization. Immunity. 2015; 42:419–430. [PubMed: 25786174]

Karplus PA, Diederichs K. Linking crystallographic model and data quality. Science. 2012; 336:1030–1033. [PubMed: 22628654]

Karplus PA, Diederichs K. Assessing and maximizing data quality in macromolecular crystallography. Curr. Opin. Struct. Biol. 2015; 34:60–68. [PubMed: 26209821]

Lampropoulou V, Sergushichev A, Bambouskova M, Nair S, Vincent EE, Loginicheva E, Cervantes-Barragan L, Ma X, Huang SC, Griss T, et al. Itaconate Links Inhibition of Succinate Dehydrogenase with Macrophage Metabolic Remodeling and Regulation of Inflammation. Cell Metab. 2016; 24:158–166. [PubMed: 27374498]

Lek M, Karczewski KJ, Minikel EV, Samocha KE, Banks E, Fennell T, O'Donnell-Luria AH, Ware JS, Hill AJ, Cummings BB, et al. Analysis of protein-coding genetic variation in 60,706 humans. Nature. 2016; 536:285–291. [PubMed: 27535533]

Lim ET, Wurtz P, Havulinna AS, Palta P, Tukiainen T, Rehnstrom K, Esko T, Magi R, Inouye M, Lappalainen T, et al. Distribution and medical impact of loss-of-function variants in the Finnish founder population. PLoS Genet. 2014; 10:e1004494. [PubMed: 25078778]

Lin X, Lu D, Gao Y, Tao S, Yang X, Feng J, Tan A, Zhang H, Hu Y, Qin X, et al. Genome-wide association study identifies novel loci associated with serum level of vitamin B12 in Chinese men. Hum. Mol. Genet. 2012; 21:2610–2617. [PubMed: 22367966]

Luan HH, Medzhitov R. Food Fight: Role of Itaconate and Other Metabolites in Antimicrobial Defense. Cell Metab. 2016; 24:379–387. [PubMed: 27626199]

MacArthur DG, Balasubramanian S, Frankish A, Huang N, Morris J, Walter K, Jostins L, Habegger L, Pickrell JK, Montgomery SB, et al. A systematic survey of loss-of-function variants in human protein-coding genes. Science. 2012; 335:823–828. [PubMed: 22344438]

McCoy AJ, Grosse-Kunstleve RW, Adams PD, Winn MD, Storoni LC, Read RJ. Phaser crystallographic software. J Appl Crystallogr. 2007; 40:658–674. [PubMed: 19461840]

McFadden BA, Purohit S. Itaconate, an isocitrate lyase-directed inhibitor in Pseudomonas indigofera. J. Bacteriol. 1977; 131:136–144. [PubMed: 17593]

Michelucci A, Cordes T, Ghelfi J, Pailot A, Reiling N, Goldmann O, Binz T, Wegner A, Tallam A, Rausell A, et al. Immune-responsive gene 1 protein links metabolism to immunity by catalyzing itaconic acid production. Proc. Natl. Acad. Sci. U. S. A. 2013; 110:7820–7825. [PubMed: 23610393]

Montgomery JA, Mamer OA, Scriver CR. Metabolism of ethylmalonate to mesaconate in the rat. Evidence for trans-dehydrogenation of methylsuccinate. Biochem. J. 1983; 214:641–644. [PubMed: 6225430]

Padovani D, Banerjee R. Alternative pathways for radical dissipation in an active site mutant of B12-dependent methylmalonyl-CoA mutase. Biochemistry. 2006a; 45:2951–2959. [PubMed: 16503649]

Padovani D, Banerjee R. Assembly and protection of the radical enzyme, methylmalonyl-CoA mutase, by its chaperone. Biochemistry. 2006b; 45:9300–9306. [PubMed: 16866376]

Padovani D, Banerjee R. A G-protein editor gates coenzyme B12 loading and is corrupted in methylmalonic aciduria. Proc. Natl. Acad. Sci. U. S. A. 2009; 106:21567–21572. [PubMed: 19955418]

Pan D, Fujimoto M, Lopes A, Wang YX. Twist-1 is a PPARdelta-inducible, negative-feedback regulator of PGC-1alpha in brown fat metabolism. Cell. 2009; 137:73–86. [PubMed: 19345188]

Patel TR, McFadden BA. Caenorhabditis elegans and Ascaris suum: inhibition of isocitrate lyase by itaconate. Exp. Parasitol. 1978; 44:262–268. [PubMed: 658222]

Sancak Y, Markhard AL, Kitami T, Kovacs-Bogdan E, Kamer KJ, Udeshi ND, Carr SA, Chaudhuri D, Clapham DE, Li AA, et al. EMRE is an essential component of the mitochondrial calcium uniporter complex. Science. 2013; 342:1379–1382. [PubMed: 24231807]

Sanjana NE, Shalem O, Zhang F. Improved vectors and genome-wide libraries for CRISPR screening. Nat Methods. 2014; 11:783–784. [PubMed: 25075903]

Sasikaran J, Ziemski M, Zadora PK, Fleig A, Berg IA. Bacterial itaconate degradation promotes pathogenicity. Nat. Chem. Biol. 2014; 10:371–377. [PubMed: 24657929]

Sastry GM, Adzhigirey M, Day T, Annabhimoju R, Sherman W. Protein and ligand preparation: parameters, protocols, and influence on virtual screening enrichments. J. Comput. Aided Mol. Des. 2013; 27:221–234. [PubMed: 23579614]

Strelko CL, Lu W, Dufort FJ, Seyfried TN, Chiles TC, Rabinowitz JD, Roberts MF. Itaconic acid is a mammalian metabolite induced during macrophage activation. J. Am. Chem. Soc. 2011; 133:16386–16389. [PubMed: 21919507]

Strittmatter L, Li Y, Nakatsuka NJ, Calvo SE, Grabarek Z, Mootha VK. CLYBL is a polymorphic human enzyme with malate synthase and beta-methylmalate synthase activity. Hum. Mol. Genet. 2014; 23:2313–2323. [PubMed: 24334609]

Taoka S, Padmakumar R, Lai MT, Liu HW, Banerjee R. Inhibition of the human methylmalonyl-CoA mutase by various CoA-esters. J. Biol. Chem. 1994; 269:31630–31634. [PubMed: 7989334]

Vlasie MD, Banerjee R. When a spectator turns killer: suicidal electron transfer from cobalamin in methylmalonyl-CoA mutase. Biochemistry. 2004; 43:8410–8417. [PubMed: 15222752]

Vonrhein C, Flensburg C, Keller P, Sharff A, Smart O, Paciorek W, Womack T, Bricogne G. Data processing and analysis with the autoPROC toolbox. Acta Crystallogr. D Biol. Crystallogr. 2011; 67:293–302. [PubMed: 21460447]

Wang SF, Adler J, Lardy HA. The pathway of itaconate metabolism by liver mitochondria. J. Biol. Chem. 1961; 236:26–30. [PubMed: 13783048]

Watkins D, Rosenblatt DS. Inborn errors of cobalamin absorption and metabolism. Am. J. Med. Genet. C Semin. Med. Genet. 2011; 157C:33–44. [PubMed: 21312325]

Watkins D, Rosenblatt DS. Lessons in biology from patients with inherited disorders of vitamin B12 and folate metabolism. Biochimie. 2016; 126:3–5. [PubMed: 27163846]

Williams JO, Roche TE, McFadden BA. Mechanism of action of isocitrate lyase from Pseudomonas indigofera. Biochemistry. 1971; 10:1384–1390. [PubMed: 5580657]

Wu C, Jin X, Tsueng G, Afrasiabi C, Su AI. BioGPS: building your own mash-up of gene annotations and expression profiles. Nucleic Acids Res. 2016; 44:D313–316. [PubMed: 26578587]

Wu C, Macleod I, Su AI. BioGPS and MyGene.info: organizing online, gene-centric information. Nucleic Acids Res. 2013; 41:D561–565. [PubMed: 23175613]

Zarzycki J, Brecht V, Muller M, Fuchs G. Identifying the missing steps of the autotrophic 3-hydroxypropionate CO2 fixation cycle in Chloroflexus aurantiacus. Proc. Natl. Acad. Sci. U. S. A. 2009; 106:21317–21322. [PubMed: 19955419]

Zarzycki J, Kerfeld CA. The crystal structures of the tri-functional Chloroflexus aurantiacus and bi-functional Rhodobacter sphaeroides malyl-CoA lyases and comparison with CitE-like superfamily enzymes and malate synthases. BMC Struct. Biol. 2013; 13:28. [PubMed: 24206647]

Highlights

- Mammalian CLYBL is a citramalyl-CoA lyase *in vitro* and in cells.
- Loss of CLYBL leads to a cell autonomous deficiency in mitochondrial B_{12}.
- CoA ester of itaconate directly inhibits MUT by poisoning the B_{12} cofactor.

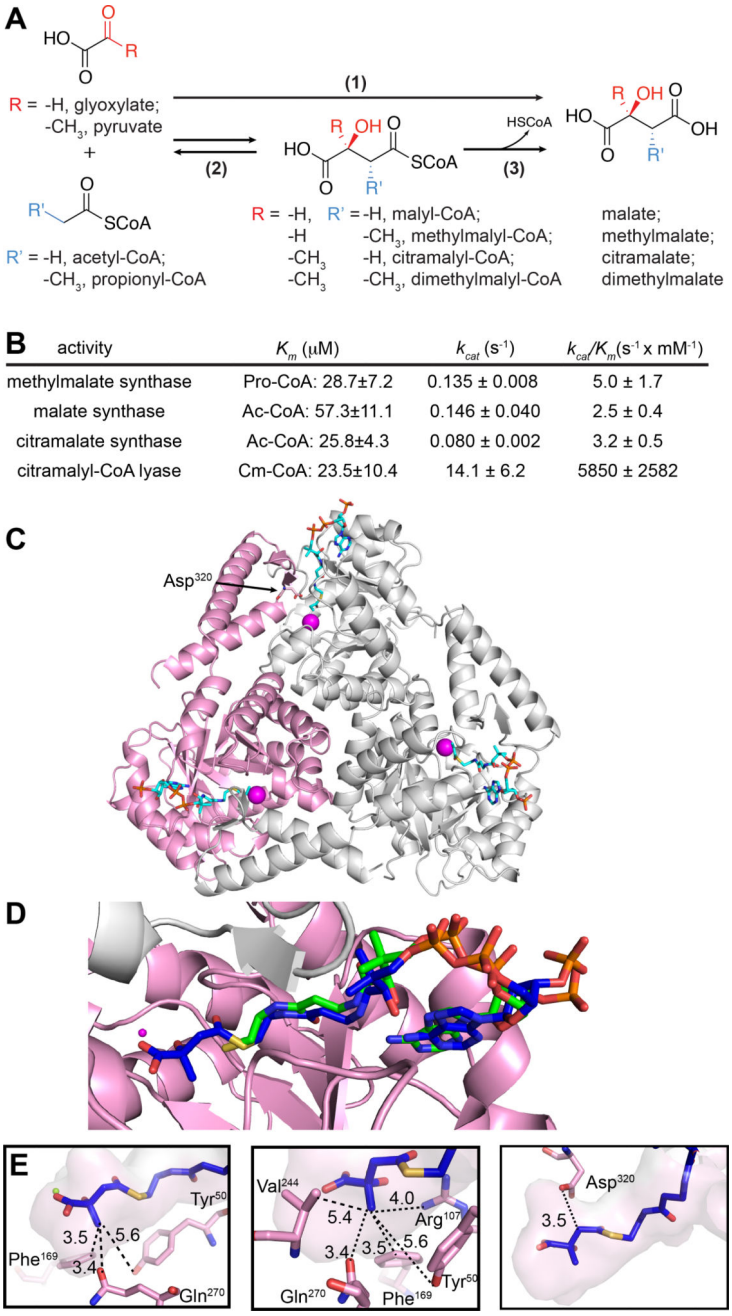

Figure 1. Enzymatic activity and crystal structure of CLYBL

(A) Putative enzymatic activities of CLYBL. We detected (1) malate/methylmalate/ citramalate synthase activity, (2) citramalyl-CoA lyase activity and (3) malyl-CoA thioesterase activity.

(B) *In vitro* enzyme analysis of CLYBL reveals high citramalyl-CoA lyase activity.

(C) Crystal structure of human CLYBL trimer. One subunit is shown in pink, magnesium ion in magenta, and the substrate mimic propionyl-CoA in cyan. The critical residue for catalytic activity Asp^{320} is highlighted.

(D) Docking of citramalyl-CoA in the substrate binding pocket of the CLYBL structure. Free CoASH in the structure is shown in green, docked citramalyl-CoA in blue, one CLYBL subunit in pink and the neighboring subunit in gray.

(E) The distances between docked citramalyl-CoA and the CLYBL residues are too close to accommodate additional carbon atoms in substrates larger than citramalyl-CoA. Three different views are shown. Labeled distances are in Angstrom (Å). The substrate-binding pocket of CLYBL is shown in surface representation.

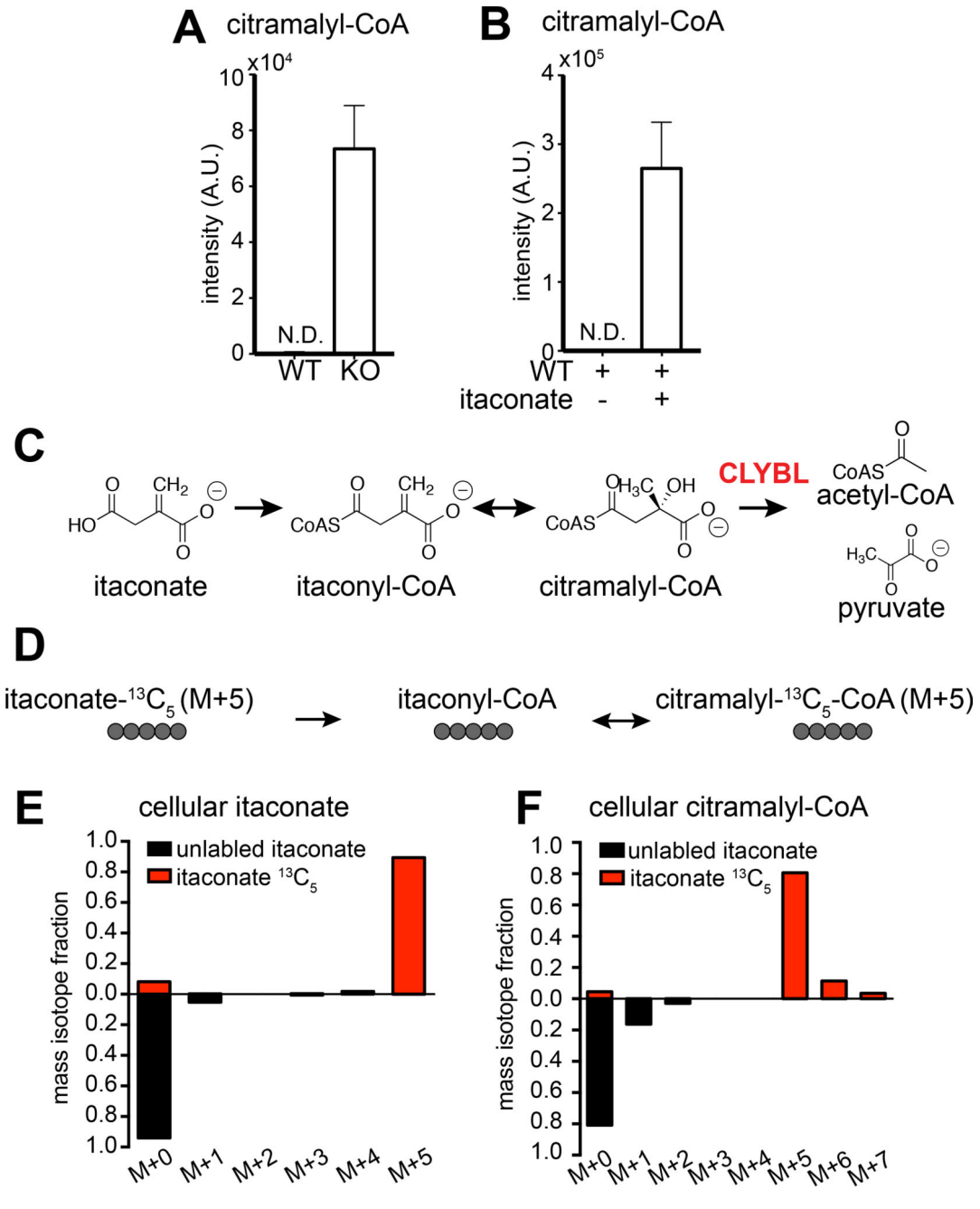

Figure 2. CLYBL is a citramalyl-CoA lyase operating in C5 dicarboxylate catabolism

(A) Citramalyl-CoA levels in extracts from control and Clybl KO brown adipocytes. All results are means ± SD (n ≥ 3 biologic replicates) and were confirmed in independent experiments.

(B) Citramalyl-CoA levels in the control brown adipocytes treated with 2 mM itaconate.

(C) Schematic of the proposed CLYBL-mediated reaction in itaconate metabolism.

(D) Schematic of itaconate -$^{13}C_5$ labeling into citramalyl-CoA.

(E) – (F) Relative abundances of different mass isotopomers of cellular itaconate (in E) and citramalyl-CoA (in F) from control brown adipocytes treated with either labeled and unlabeled itaconate.

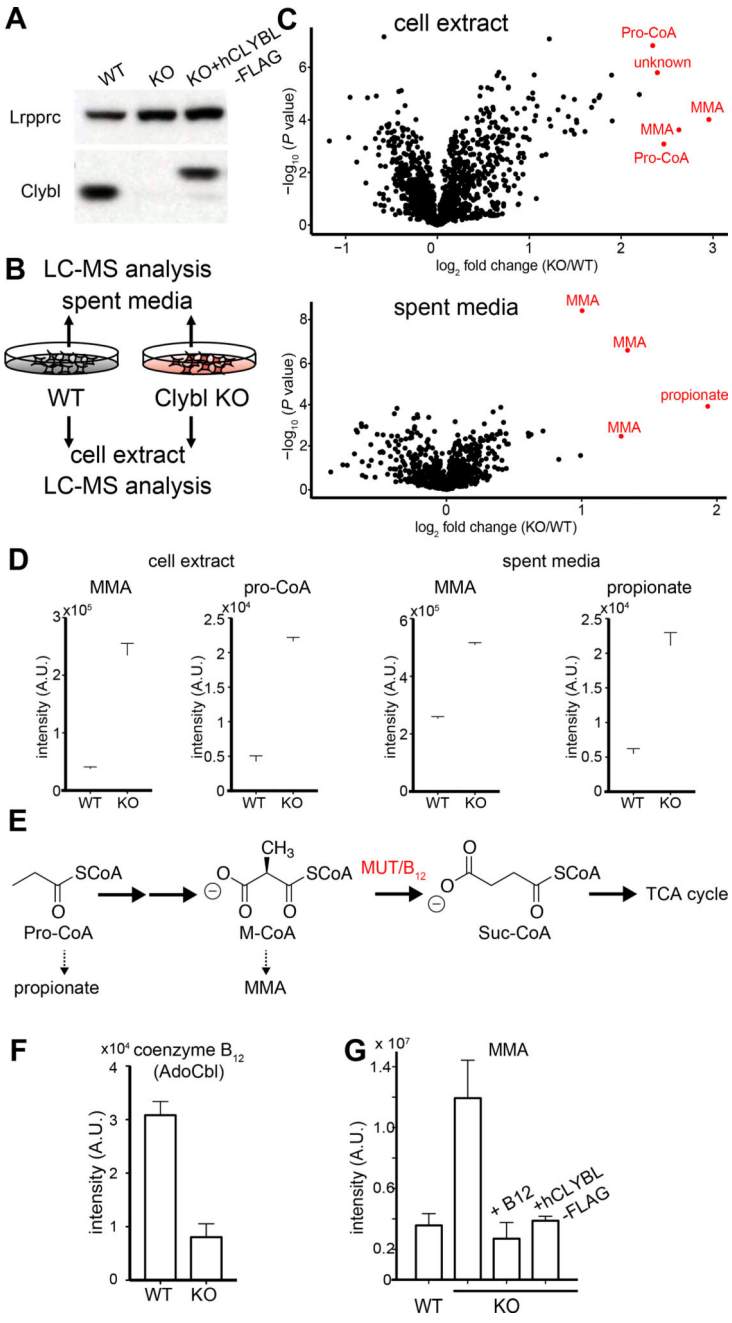

Figure 3. Loss of CLYBL leads to a cell-autonomous defect in mitochondrial B_{12} metabolism

(A) Western blot of Clybl in Clybl CRISPR KO murine brown adipocytes and Clybl KO cells expressing FLAG-tagged human CLYBL.

(B) Schematic of the LC-MS-based untargeted metabolomics experiment design.

(C) Volcano plot of the steady state level of metabolite ions from 3 d spent media and cellular extract from Clybl KO brown adipocytes and controls.

(D) Bar graphs showing the change of the mitochondrial B_{12} pathway metabolites in Clybl KO brown adipocytes.

(E) Schematic of the mitochondrial B_{12} metabolic pathway.

(F) Coenzyme B_{12} level in Clybl KO brown adipocytes and controls.
(G) Methylmalonate (MMA) accumulation in Clybl KO cellular extract can be reversed by excess vitamin B_{12} in the media (500 nM) or re-expressing human CLYBL that is resistant to the CRISPR reagent.

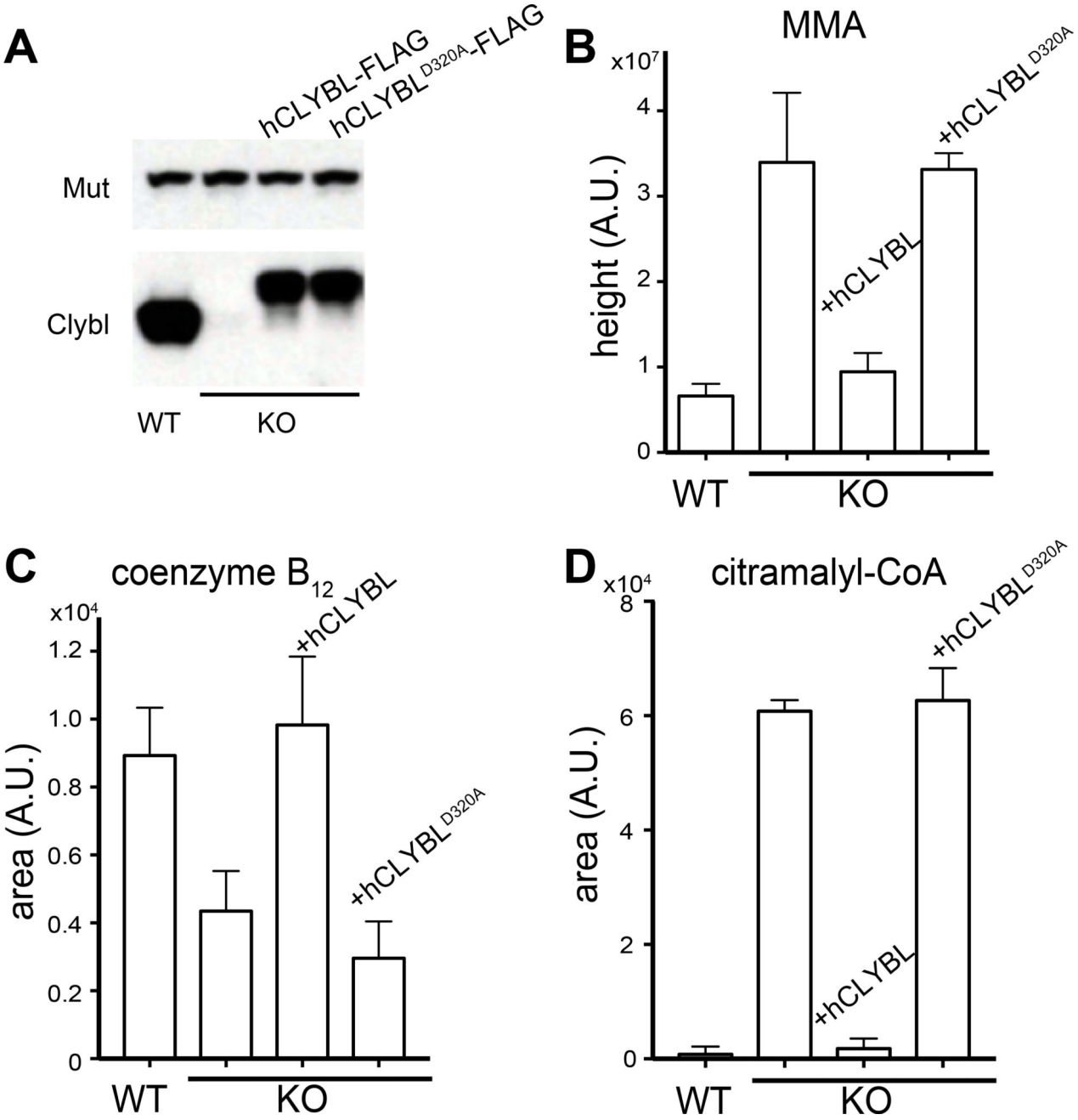

Figure 4. Enzyme activity of CLYBL is required to support mitochondrial B_{12} in brown adipocytes

(A) Western blot of FLAG-tagged wild type human CLYBL and catalytic dead mutant $CLYBL^{D320A}$ in Clybl KO cells.

(B–D) Methylmalonate (MMA) accumulation (in B), coenzyme B_{12} inhibition (in C), and citramalyl-CoA accumulation (in D) in Clybl KO cellular extract cannot be rescued by catalytically dead mutant of CLYBL.

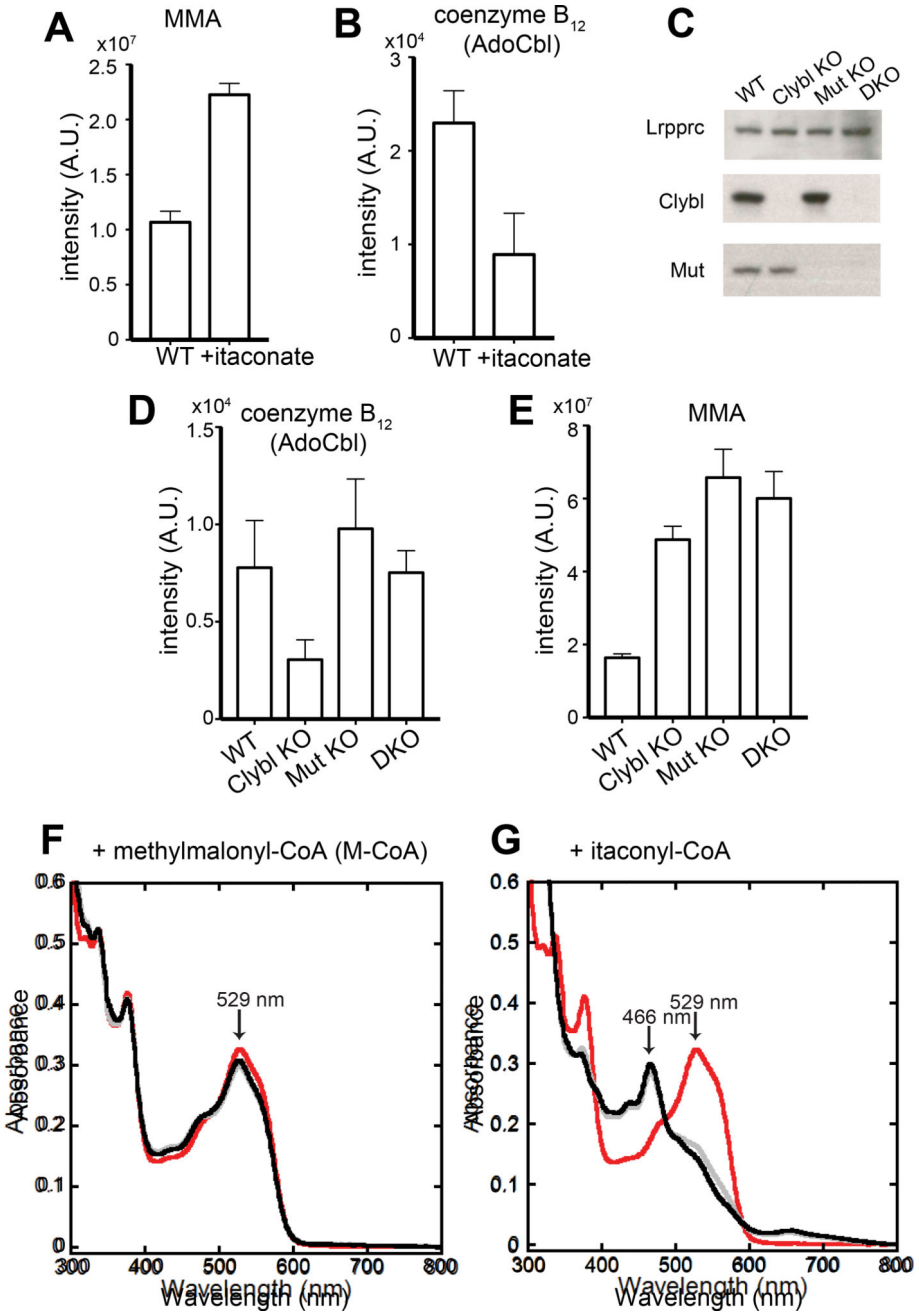

Figure 5. Itaconyl-CoA directly inactivates coenzyme B12 through MUT

(A) Cellular methylmalonate (MMA) is accumulated in control brown adipocytes treated with 2 mM itaconate.

(B) Coenzyme B_{12} is reduced in control brown adipocytes treated with 2 mM itaconate.

(C) Western blot of Clybl, Mut in double KO cells.

(D–E) Loss of Mut suppresses coenzyme B_{12} deficiency in Clybl KO cells (in D), despite similarly increased MMA level (in E), suggesting that the inhibition mechanism is via MUT activity. (F–G) Itaconyl-CoA inactivates human MUT enzyme. Purified human MUT enzyme was preloaded with coenzyme B_{12} AdoCbl (with an absorbance maximum at 529

nm). UV-visible spectra were recorded before (red), immediately after (gray), and 20 min after (black) addition of either substrate M-CoA (in F) or itaconyl-CoA (in G). Unlike M-CoA, which elicited only minor spectral changes, itaconyl-CoA triggered a large blue shift in the absorbance maximum to 466 nm, indicating formation of inactive cob(II)alamin.

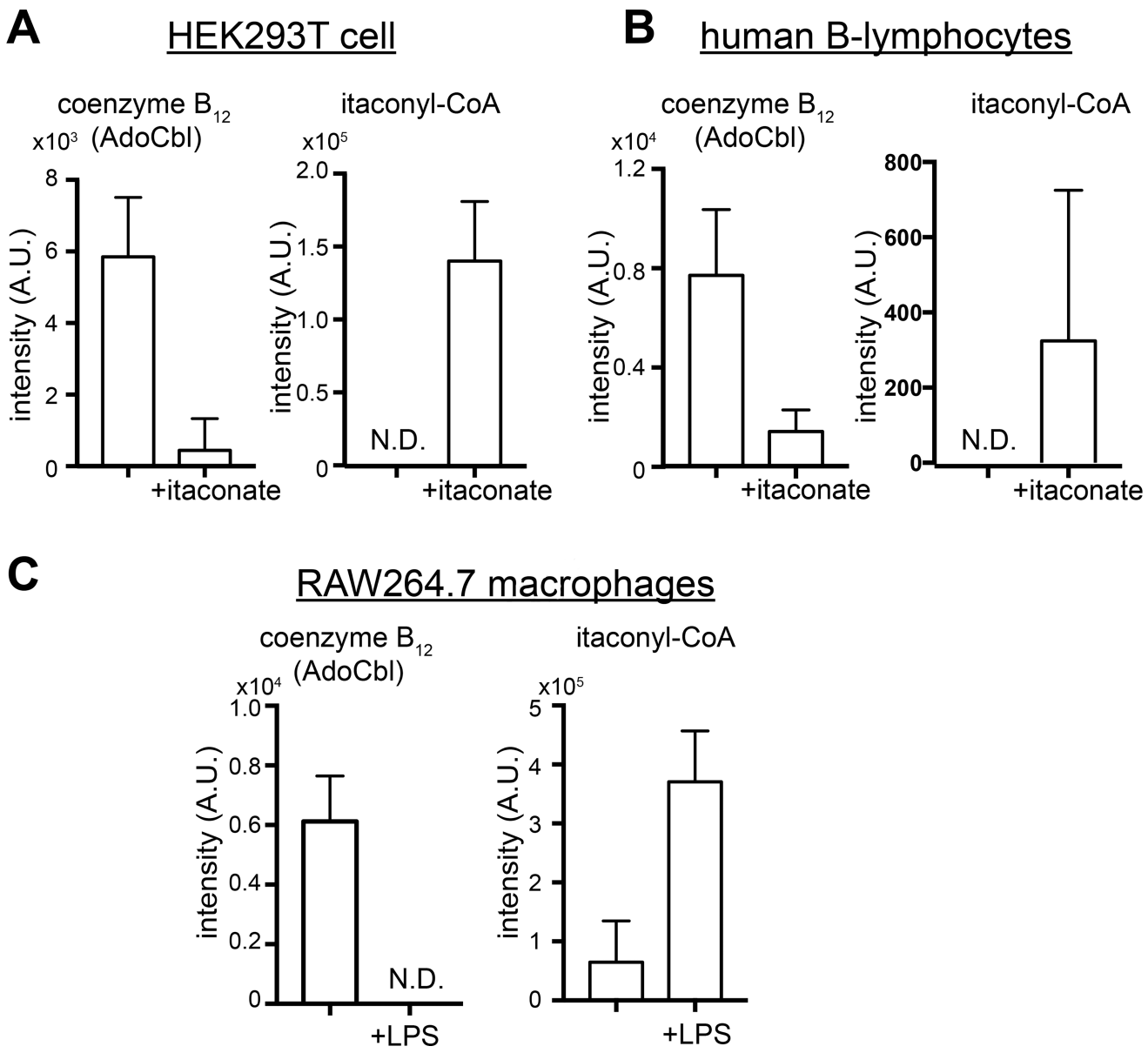

Figure 6. The immunomodulatory metabolite itaconate poisons vitamin B12 in various cell types

(A–B) Coenzyme B_{12} is reduced by 2 mM itaconate treatment in HEK293T cell (in A), and in human B-lymphocytes (in B). Itaconyl-CoA is undetected in untreated cells, but dramatically increased in treated cells.

(C) Coenzyme B_{12} is ablated in macrophages upon 10 ng/ml LPS stimulation for 6 hr. Itaconyl-CoA is dramatically increased upon stimulation.

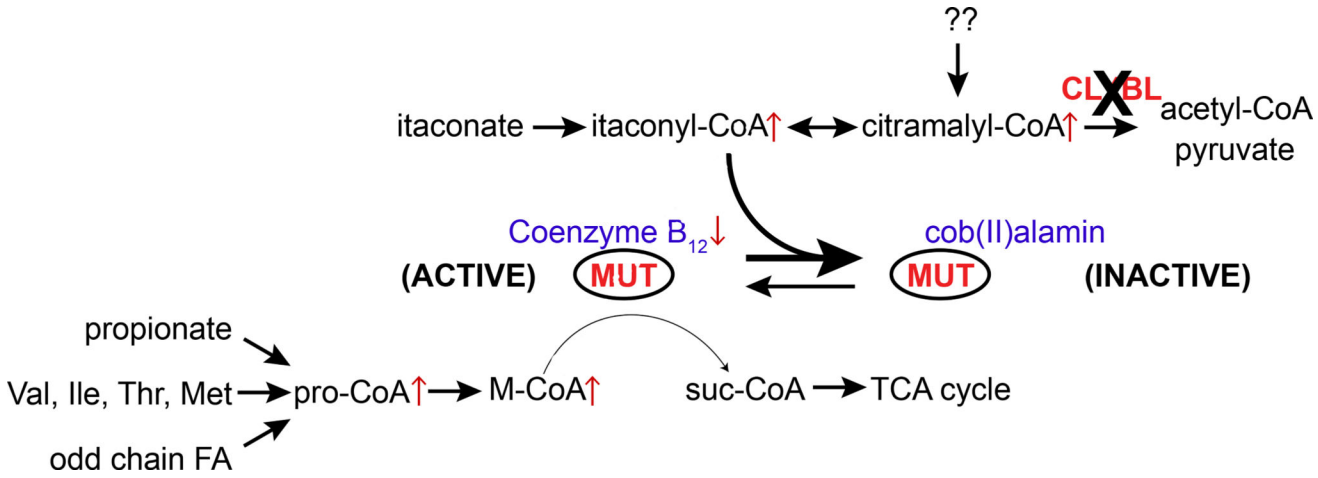

Figure 7. Relationship between CLYBL, itaconate and B_{12}

CLYBL functions as a citramalyl-CoA lyase, and its loss leads to an accumulation of upstream metabolites. Itaconyl-CoA serving as a substrate analog directly inhibits the MUT enzyme and rapidly inactivates the coenzyme B_{12}.